ADVANCED MATERIALS
www.advmat.de

Recent Progress in Flexible Tactile Sensors for Human-Interactive Systems: From Sensors to Advanced Applications

*Soonjae Pyo, Jaeyong Lee, Kyubin Bae, Sangjun Sim, and Jongbaeg Kim**

Flexible tactile sensors capable of measuring mechanical stimuli via physical contact have attracted significant attention in the field of human-interactive systems. The utilization of tactile information can complement vision and/or sound interaction and provide new functionalities. Recent advancements in micro/nanotechnology, material science, and information technology have resulted in the development of high-performance tactile sensors that reach and even surpass the tactile sensing ability of human skin. Here, important advances in flexible tactile sensors over recent years are summarized, from sensor designs to system-level applications. This review focuses on the representative strategies based on design and material configurations for improving key performance parameters including sensitivity, detection range/linearity, response time/hysteresis, spatial resolution/crosstalk, multidirectional force detection, and insensitivity to other stimuli. System-level integration for practical applications beyond conceptual prototypes and promising applications, such as artificial electronic skin for robotics and prosthetics, wearable controllers for electronics, and bidirectional communication tools, are also discussed. Finally, perspectives on issues regarding further advances are provided.

1. Introduction

Tactile sensation, an important function of human skin, can assist interaction with the surrounding environment via physical contact. Specialized tactile receptors respond to external stimuli, such as pressure, bending, stretching, and temperature change; therefore, humans can recognize the contacted object.[1] To emulate the pressure-sensing capability of the human skin, which is the most representative sensory function, tactile sensors that can perceive and quantify mechanical stimuli by transducing applied stimulus into electronic signals have been proposed. Tactile sensors are generally based on touch/pressure detection; furthermore, mechanisms or devices to detect other stimuli, such as strain, temperature, and humidity, may be integrated. A tactile feedback system, integrated with a prosthetic hand, was demonstrated in 1974,[2] and since then, a variety of tactile sensors have been actively developed for use in various applications, such as touch screens and robotic hands. However, the sensing performances of conventional tactile sensors are insufficient to achieve the outstanding perceptive features of human skin with high sensitivity, high spatial resolution, and rapid response time. Furthermore, because they comprise rigid materials such as silicon and metal thin film, mounting them on curved or soft surfaces is difficult, thereby significantly limiting their applications.

Over the past decade, considerable progress in the fields of nanomaterials and micro/nanomanufacturing has accelerated the development of flexible electronics, especially tactile sensors. Various flexible tactile sensors, based on different transduction mechanisms including resistive, capacitive, piezoelectric, and triboelectric types, with improved performances have been explored.[3] For example, conventional capacitive tactile sensors comprising two facing metal electrodes and a dielectric elastomer between them had limitations such as insufficient flexibility, low sensitivity, and slow response time. To enhance the flexibility of capacitive tactile sensors and achieve stretchability and transparency, Lipomi et al. utilized stretchable carbon nanotube (CNT) film as an electrode material instead of metal, and successfully demonstrated a flexible/stretchable and highly transparent tactile sensor array.[4] Engineering the dielectric layer via an unusual fabrication technique was also proposed to improve the sensitivity and response time.[5] The tactile sensor with a microporous dielectric exhibited significantly higher sensitivity and faster response time than the conventional unstructured tactile sensor. Furthermore, several approaches based on novel materials, designs, and manufacturing methods have been devised to enhance sensor performances, such as sensitivity, detection range, linearity, response time, spatial resolution, and to provide new functionalities such as multidirectional force detection and screening environmental effects.

In addition to performance improvement, the integration of tactile sensors with various functional components has attracted significant attention on the following aspects: 1) multisensory

Prof. S. Pyo
Department of Mechanical System Design Engineering
Seoul National University of Science and Technology
232 Gongneung-ro, Nowon-gu, Seoul 01811, Republic of Korea

J. Lee, K. Bae, S. Sim, Prof. J. Kim
School of Mechanical Engineering
Yonsei University
50 Yonsei-ro, Seodaemun-gu, Seoul 03722, Republic of Korea
E-mail: kimjb@yonsei.ac.kr

The ORCID identification number(s) for the author(s) of this article can be found under https://doi.org/10.1002/adma.202005902.

DOI: 10.1002/adma.202005902

systems for simultaneously detecting strain, temperature, humidity, and pressure were developed to provide improved interaction between humans and machines; 2) self-powered sensors or flexible energy storage devices were utilized to realize self-sustainable tactile-sensing systems; and 3) wireless communication modules were integrated onto tactile sensors to enable signal processing and data transmission in real time. With recent advances in performance improvement and system-level integration of flexible tactile sensors, their applications have increased.[6,7] One of the promising applications of tactile sensors is the human-interactive system, which allows a human to communicate with humans or machines via tactile sensation. To date, remote activities using an exploratory robot have been limited because it relied only on visual (camera-screen) and sound perception (microphone-speaker). In contrast, tactile feedback system with tactile sensors and displays can enable more delicate and complicated operation, for example, manipulation of fragile objects and investigation of material properties. In addition, wearable tactile sensors are expected to play important roles as real-time interactive devices in virtual or augmented reality (VR/AR) communication, which is a key technology in the fourth industrial revolution. Therefore, several researchers have demonstrated proof-of-concept tactile feedback systems and control interfaces, validating the potential utility of tactile sensors.[8,9]

Recently, several reviews have extensively covered the progress in transduction mechanisms, materials, and manufacturing of flexible tactile/pressure sensors for various applications such as electronic skins (e-skins), biomedical applications, and advanced intelligent systems.[10–15] Therefore, this review focuses on the detailed strategies for enhancing key performances of flexible tactile sensors for touch/pressure detection and their system-level integration for human-interactive systems (**Figure 1**). In the first section, we briefly highlight the

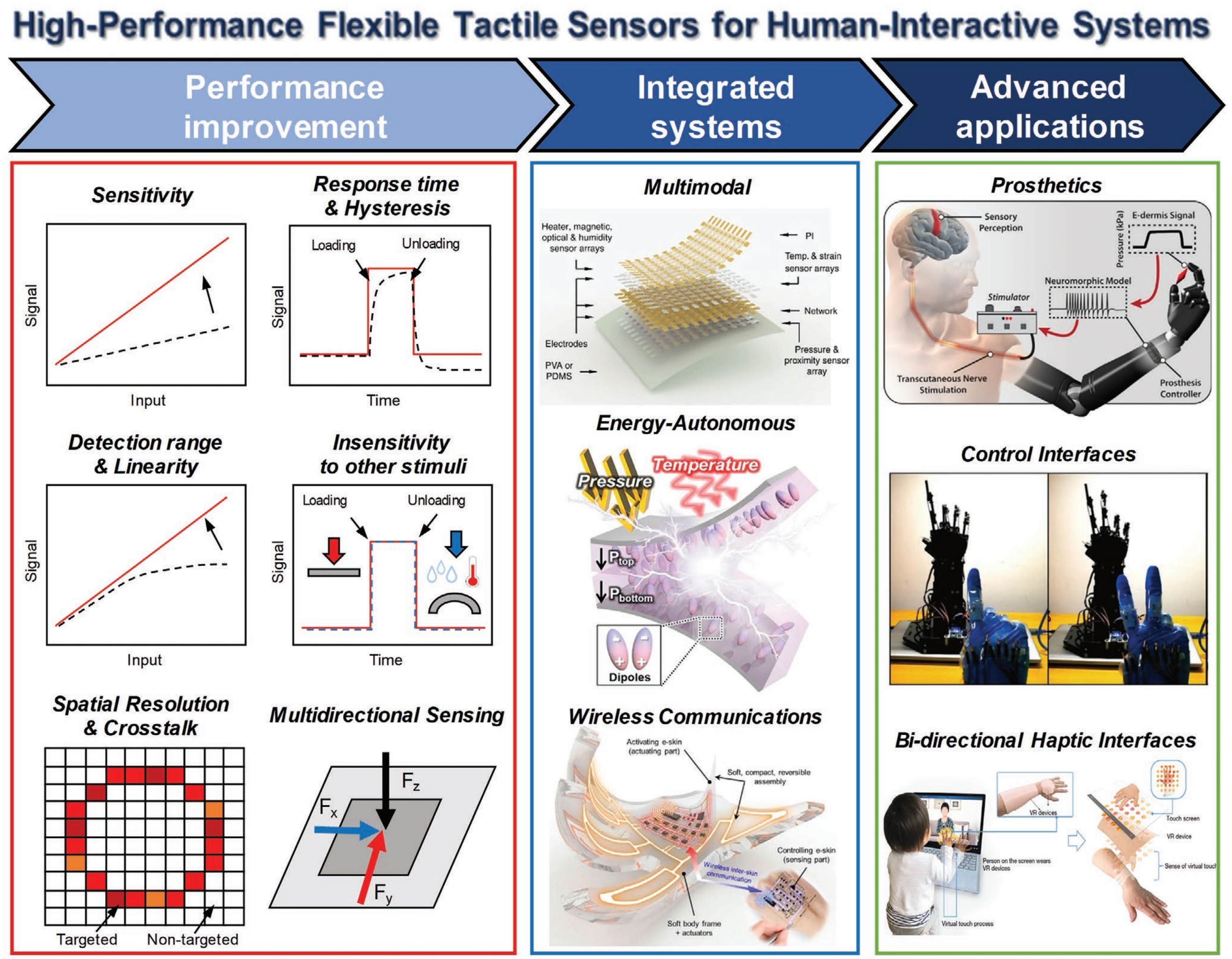

Figure 1. Overview of the review. i) Progress in tactile sensors in terms of sensing performances. ii) Designs for integrating high-performance tactile sensors for multimodal, energy-autonomous, and wireless sensing platforms. Multimodal: Reproduced with permission.[112] Copyright 2018, Springer Nature. Energy-auonomous: Reproduced with permission.[134] Copyright 2020, Elsevier Ltd. Wireless communication: Reproduced with permission.[182] Copyright 2018, AAAS. iii) State-of-the-art applications of tactile sensing in prosthetics, control interfaces and bidirectional user interfaces. Prosthetics: Reproduced with permission.[176] Copyright 2018, AAAS. Control interfaces: Reproduced with permission.[180] Copyright 2018, Springer Nature. Bidirectional haptic interfaces: Reproduced with permission.[187] Copyright 2019, Springer Nature.

widely used transduction mechanisms of tactile sensors. Then, an overview of the performance parameters and the representative approaches for improving them are provided. The state-of-the-art strategies for integrated tactile sensor systems, including multimodal sensor systems, energy-autonomous systems, and wireless communication are discussed in the third section. The fourth section presents the applications of tactile sensors in human-interactive systems, for example, artificial e-skin, control interfaces, and interactive tactile interfaces. Finally, we summarize the recent developments in flexible tactile sensors and discuss the crucial issues that must be addressed for practical applications that are beyond conceptual prototypes.

2. Transduction Principles of Tactile Sensors

Tactile sensors transduce applied pressure into an electrical signal, facilitating the detection of the magnitude and/or direction of the pressure by measuring the signal change. Although various transduction mechanisms have been studied, the most widely used mechanisms in flexible tactile sensors include resistive, capacitive, and piezoelectric types. Recently, tactile sensors based on the triboelectric effect have attracted significant interest owing to their simple structure and energy-harvesting capability. Each of these transduction mechanisms has unique characteristics, based on different materials and structures. Herein, we briefly introduce the basic structure, most widely used materials, and operating principles for each mechanism.

2.1. Resistive Tactile Sensors

The fundamental principle of the resistive tactile sensor is the transduction of external pressure into a change in electrical resistance. Unlike conventional piezoresistive sensors exploiting the strain-induced change in electrical resistivity (piezoresistivity), resistive sensors rely on the change in contact resistance. Resistive tactile sensors comprise active materials sandwiched between two opposing electrodes or stacked on a pair of in-plane electrodes. The active materials are generally in the form of composite that is composed of conductive materials and matrix. When pressure is applied to the sensor, the contacts between conductive materials in a porous matrix or the contact area between the conductive materials and electrodes increases, thereby considerably decreasing the resistance. The composition and geometric design of the active material are important drivers of the performance of the tactile sensor because it serves as both an electrical pathway for current flow and a deformable structure during operation. Diverse nanomaterials have been studied for use as a conductive material, that is, 0D materials (e.g., metal nanoparticles[16]), 1D materials [e.g., metal nanowires (NWs)[17] and CNTs[18]], and 2D materials (e.g., reduced graphene oxide (rGO)[19] and MXene[20]). As a matrix component, various polymers (polydimethylsiloxane (PDMS)[21] and Ecoflex[22]) and textiles (cotton[23] and polyester[24]) have been used. Resistive tactile sensors have advantages such as high sensitivity, simple device structure, and a facile fabrication process; however, high power consumption is regarded as drawbacks.

2.2. Capacitive Tactile Sensors

Capacitive type is one of the most common mechanisms used in tactile sensing. Capacitive tactile sensors, which transduce pressure input into a change in the capacitance, are typically fabricated by sandwiching a dielectric layer between two parallel electrodes. Under applied voltage, the opposite charges on the electrodes yield a capacitor and the corresponding capacitance (C) can be expressed by $C = \varepsilon_0 \varepsilon_r A/d$, where ε_0 is the permittivity of vacuum, ε_r is the relative permittivity of the dielectric layer, A is the overlapping area between the two electrodes, and d is the distance between the electrodes. The capacitance of tactile sensors can be changed under pressure owing to the geometrical changes. Among the three variables that are responsive to changes in pressure (ε_r, A, and d), d and A are typically utilized to measure the normal and shear forces, respectively. Recently, capacitive tactile sensors, utilizing the pressure-dependent permittivity, were also proposed.[25] To date, a variety of conductive materials such as metal NWs,[26] indium tin oxide (ITO),[27] CNTs,[4] and graphene,[28] have been used as electrode materials for flexible capacitive tactile sensors. For dielectric layers, various elastomers with a low modulus, for example, PDMS,[29] polyurethane,[30] and Ecoflex,[25] have been explored. Capacitive tactile sensors exhibit low power consumption, temperature independence, and stability against long-term signal drift. However, they are highly susceptible to electromagnetic interference and require a complex measurement circuit.

2.3. Piezoelectric Tactile Sensors

The fundamental principle of the piezoelectric tactile sensor is based on the piezoelectric effect, where deformation generates voltage due to electric dipole moments. Piezoelectric sensors typically consist of two parallel electrodes and a piezoelectric material between them, and external pressure causes the piezoelectric material to deform. The deformation results in a change in the dipole density, which leads to a voltage generation. The generated voltage depends on the amount of deformation; therefore, the magnitude of the applied pressure can be detected by measuring the voltage. Among the available piezoelectric materials, polyvinylidene fluoride (PVDF),[31] zinc oxide (ZnO),[32] and lead zirconate titanate (PZT)[33] have been adopted for tactile sensing. Tactile sensors based on PVDF and its composite have attracted interest owing to the mechanical flexibility, ease of fabrication, and low cost of PVDF. Piezoelectric tactile sensors exhibit high sensitivity and excellent dynamic response, making them promising candidates for the detection of dynamic pressure such as vibration detection and texture characterization. In contrast, the detection of static pressure is limited because the piezoelectric effect occurs only when the applied stimuli change.

2.4. Triboelectric Tactile Sensors

A triboelectric generator (TENG) was developed in 2012,[34] based on the coupling of triboelectric and electrostatic effects. TENGs have great potential significance as harvesters and sensors owing to their simple structure, ease of fabrication, and scalability. TENGs consist of two materials with different electronegativities covered with electrodes and generate electrical voltage through the contact and separation processes between them. This characteristic offers the choice of numerous materials, including metals, plastics, rubbers, elastomers, and textiles. Because the generated voltage of these harvesters is affected by the change in the contact area between two materials, the TENG can be utilized as a tactile sensor.[35] For triboelectric tactile sensors, various materials such as polymers (PDMS,[36] PU,[37] and polytetrafluoroethylene [PTFE][38]), hydrogels,[39] ITO,[40] and fabrics[41] have been used. Similar to piezoelectric tactile sensors, the output signal of the triboelectric sensors depends on both the magnitude and frequency of pressure, rendering them suitable for dynamic pressure sensing.

2.5. Other Types of Tactile Sensors

In addition to these representative types, several other transduction mechanisms have been explored for tactile sensing. Optical tactile sensors are based on the combination of light emitters and photodetectors, whereby the photodetector measures the changes in the intensity or wavelength of light induced by external pressure.[42] Although these sensors usually exhibit a high resolution, integration complexity and considerable power consumption for light generation limit their applications. Another type is a magnetic tactile sensor utilizing the Hall effect or giant magnetoresistance.[43] In these sensors, magnetic flux changes with applied pressure, and the magnitude or direction of the pressure can be detected by measuring the electrical signals. Magnetic sensors can detect multidirectional forces even with a single sensor unit, but they are vulnerable to noise. Recently, iontronic tactile sensors, exploiting the electron double layer (EDL) at the interface between the ionic material and electrode have been developed.[44] The transduction mechanism of the iontronic sensor is based on the change in the EDL capacitance induced by external deformation. Researches are being conducted actively to understand the mechanism of iontronic sensors and improve their performances.

3. Designs and Strategies to Enhance Sensor Performance

When designing tactile sensors, performance parameters such as sensitivity, detection range, response time, and spatial resolution should be considered to obtain precise information from the sensor-object interfaces. Performance requirements are highly dependent on target applications and thus it is difficult to provide specific requirements. Nevertheless, the pressure-sensing properties of human skin can be good references (**Table 1**) because the fundamental goal of tactile sensors is to emulate the capabilities of human skin.[1,45,46] In addition to the properties presented in Table 1, linearity, hysteresis, crosstalk, multidirectional sensing capability, and insensitivity to other stimuli must be taken into account to realize an ideal tactile sensor. In this section, we discuss key performance metrics mentioned above and highlight recent studies aimed at achieving or improving them.

Table 1. Pressure-sensing properties of human skin.

Parameter	Human skin
Sensitivity	Detection threshold: 1 mN[1]
Detection range	>10 kPa[45]
Response time	≈15 ms[1]
Spatial resolution	1 mm[46]

3.1. Sensitivity

Sensitivity is one of the prime parameters for tactile sensors because it is related to low detection limits, and fine discrimination between applied pressures, which is critical in subtle-pressure detection and measurement accuracy. Sensitivity of pressure sensors is measured from the relative change in output signals such as current, capacitance, and voltage, in response to external stimuli. For example, the sensitivity of resistive pressure sensors is generally denoted as $(\Delta I/I_0)/P$, where ΔI, I_0, and P denote the change in current, initial current, and input pressure, respectively. Extensive studies on tactile sensors have focused on various approaches to improving sensitivity.

One of the widely used strategies to enhance sensitivity is engineering microstructures such as pyramids,[47–49] porous structures,[5,50,51] and pillars[52,53] of polymeric materials that can induce large deformation under subtle external stimuli. For example, Yang et al. demonstrated highly sensitive capacitive tactile sensors based on a porous pyramid dielectric elastomer.[29] Porous materials have a low compressive modulus; therefore, the deformation of dielectrics, which leads to the capacitance change, occurs easily. Moreover, due to the pyramid structures, applied stress is concentrated on the apex, further decreasing the effective compressive modulus, and increasing the sensitivity of the sensors (**Figure 2**a). The sensor achieved a sensitivity of 44.5 kPa^{-1} under 100 Pa of pressure with a detection limit of 0.14 Pa. Chen and coworkers reported enhanced sensitivity of piezoelectric tactile sensors designed with micropillar arrays.[53] Due to the strain confinement effect, micropillars deform more under a given pressure than the planar film structure, which causes a larger output voltage (Figure 2b). Consequently, the sensitivity was enhanced to 228.2 mV N^{-1}, which is 3.3 times higher than that of the planar film counterpart. The ease of deformation of materials with such microstructures has been leveraged for developing transistor-based sensors utilizing the change in contact resistance at semiconductor–conductor interfaces (Figure 2c).[49] The sensors consist of organic semiconductors in contact with drain and source electrodes deposited on PDMS micropyramids. The pressure-induced deformation of pyramids increases the contact between the semiconductor and electrodes, reducing the contact resistance and effective channel resistance, and increasing the source–drain current. The reference device with a flat PDMS showed no apparent response to pressure, validating the effect of the microstructured design. The low initial current from the low conductivity of semiconductors and the significant change in output current and resistance at the interface enhanced sensor sensitivity (514 kPa^{-1} in 30–200 Pa; detection limit of 10 Pa), and the sensing properties could be tuned by modifying the bias conditions.

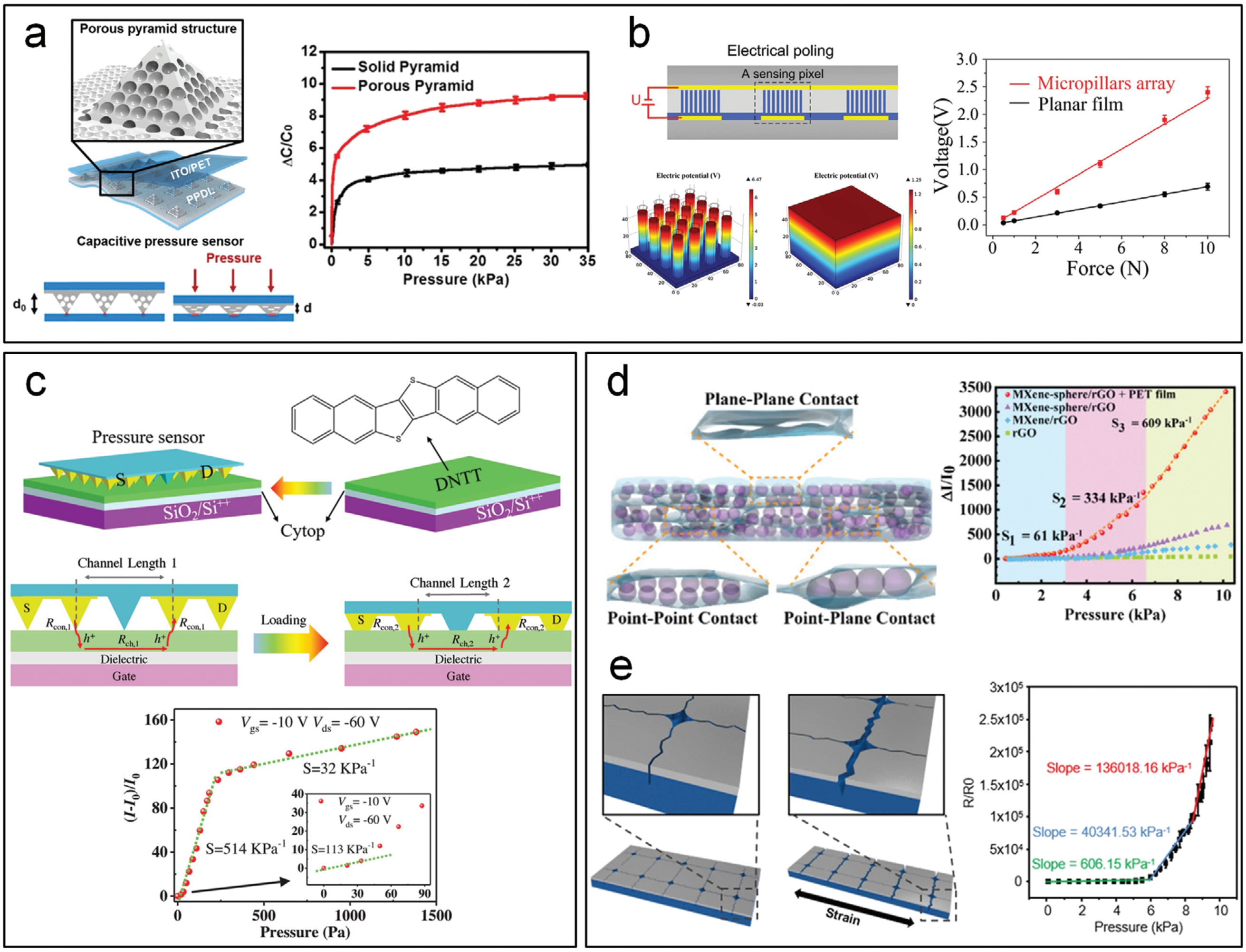

Figure 2. Representative strategies to achieve high sensitivity. a,b) Tactile sensors with a) microstructured porous pyramid and b) micropillar array, showing enhanced sensitivity than sensors without structures. (a) Reproduced with permission.[29] Copyright 2019, American Chemical Society; (b) Reproduced with permission.[53] Copyright 2020, Wiley-VCH. c) Pressure sensor based on the change in contact resistance between organic semiconductor and pyramidical structured electrodes. Reproduced with permission.[49] Copyright 2018, Wiley-VCH. d,e) Highly sensitive resistive tactile sensors with d) multiple modes of contact and e) induced mechanical cracks between sensing materials. (d) Reproduced with permission.[20] Copyright 2019, Wiley-VCH. e) Reproduced with permission.[56] Copyright 2017, Springer Nature.

Designing significant changes in the contact area between sensing materials is another possible route to increase sensitivity, especially for resistive-type sensors utilizing the change in contact resistance.[20,54–56] For example, pressure sensors based on interlocked ZnO microparticles with high-density, high-aspect-ratio nanostructured spines showed high sensitivity (75–121 kPa^{-1} in 0–200 Pa range), and a minimum detection limit of 0.015 Pa owing to signal amplification via the synergetic effect of the increased contact points between the spines and a piezoresistive effect from the bending of the spines.[54] Zhu et al. reported highly sensitive resistive tactile sensors (61–609 kPa^{-1} in 0–10 kPa range; detection limit of 6 Pa) based on hollow MXene spheres introduced into rGO aerosols that provide different modes of contact under pressure: point-to-point, point-to-plane, and plane-to-plane (Figure 2d).[20] Since mechanical disconnection dramatically reduces the conductive network even under subtle stimuli, inducing mechanical crack junctions can also be used for developing ultra-sensitive tactile sensors with a low detection limit.[55] Forming guided, straight cracks on the metal electrodes, Choi et al. demonstrated ultra-sensitive pressure sensors based on the propagation and reconnection of cracks.[56] When pressure is applied, crack propagation of the materials drastically increases the electrical resistance, and the sensors showed sensitivities of 606.15, 40 341.53, and 136 018.16 kPa^{-1} in pressure ranges of 0–6, 6–8, and 8–9.5 kPa, respectively (Figure 2e). The high sensitivity allows the sensor to detect the weight of an ant (1 mg), which corresponds to 0.2 Pa.

3.2. Detection Range and Linearity

Detection range is another key parameter in designing tactile sensors, and the specific requirements are highly dependent on applications. Pressures generated by the human body, for

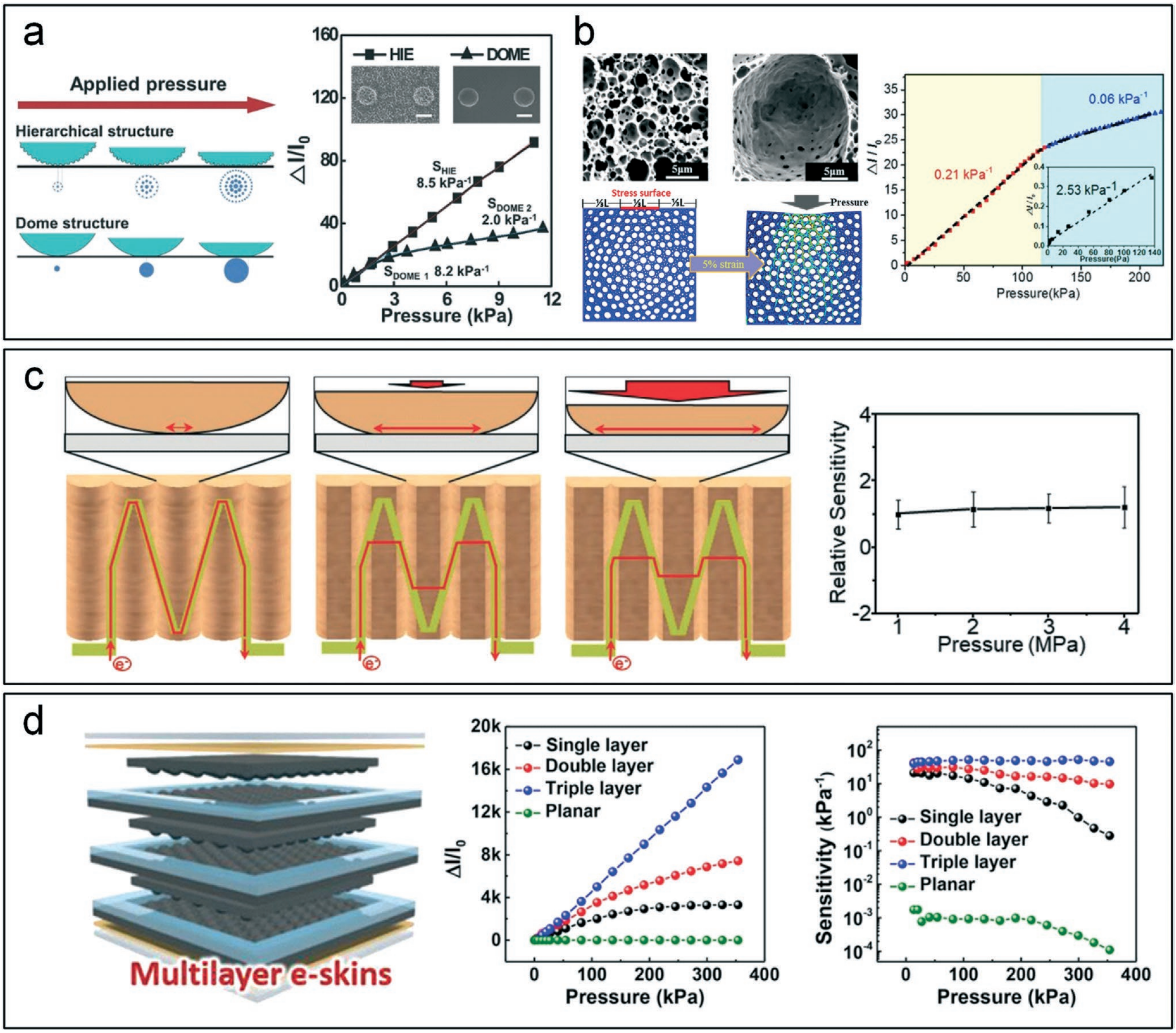

Figure 3. Tactile sensors with linearity in a broad pressure range. a,b) Tactile sensors with a) hierarchically structured graphene/PDMS array and b) hierarchically porous reduced graphene oxide/PolyHIPE foam demonstrating linear responses to pressure. (a) Reproduced with permission.[61] Copyright 2016, Wiley-VCH. (b) Reproduced with permission.[60] Copyright 2019, American Chemical Society. c) Pressure sensors based on deformation-induced lenticular contacts on designated electrodes, showing constant linearity over a wide pressure range. Reproduced with permission.[62] Copyright 2019, Wiley-VCH. d) E-skin with multilayer structures exhibiting enhanced linearity than single and double-layered devices. Reproduced with permission.[58] Copyright 2018, American Chemical Society.

example, vary from the subtle pressures of respiration (<1 kPa) and pulsation (1–10 kPa) to the large pressures of touch and motion (>10 kPa).[57,58] Therefore, achieving high sensitivity within a wide range of pressures is required for tactile sensors, especially those targeting universal applications. Linearity, which indicates how proportional the signal is relative to the applied stimulus,[59] is also highly desirable because high linearity facilitates signal processing and calibration. Many sensors experience a trade off in sensitivity and linear operational range. Sensors with high sensitivity are only operable in a limited pressure range, and sensors that can detect a broad range of pressures suffer from high nonlinearity and unstable responses in low-pressure regimes.[60] Therefore, intensive research has been conducted on increasing the sensitivity of tactile sensors over a broad linear range.

One promising method is to utilize structured materials that result in a gradual increase in contact or deformation under applied stimuli.[60–63] For instance, tactile sensors achieving a high sensitivity of 8.5 kPa^{-1} in a broad linear range up to 12 kPa were demonstrated based on a hierarchical structure where protuberances were fabricated on the arrayed, microdome-structured PDMS surfaces (**Figure 3**a).[61] When pressure is applied, the number of contact points on the material surface increases while each bump deforms, increasing the contact area. These effects made the change in total contact area linearly proportional to the applied pressure, enhancing the linearity of

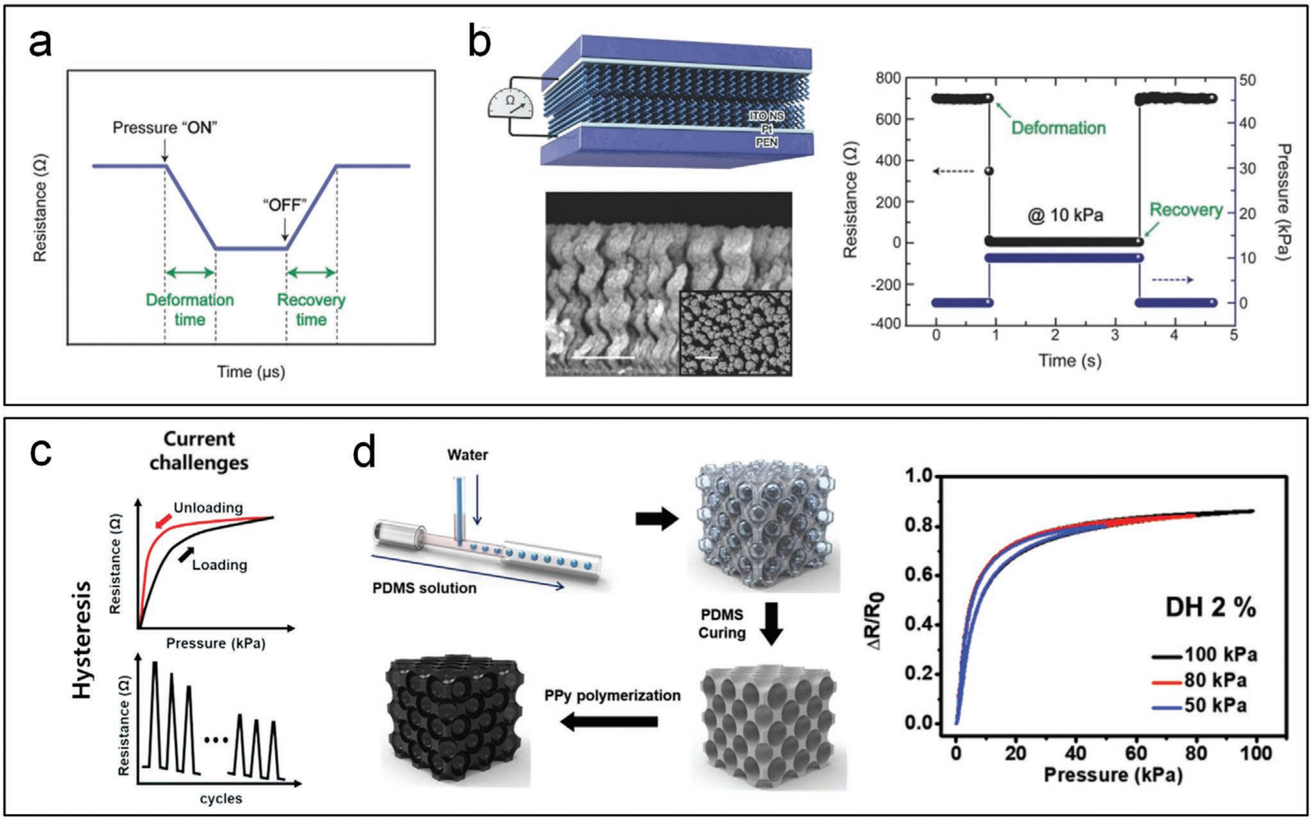

Figure 4. Approaches for reducing response time and hysteresis. a) Schematics of the "ON" and "OFF" response of resistive pressure sensor. b) Tactile sensor with a fast response based on interlocking arrays of indium tin oxide nanosprings. Reproduced with permission.[68] Copyright 2018, Wiley-VCH. c) Challenges of resistive pressure sensors from hysteresis. d) Resistive pressure sensors with low hysteresis based on chemically bonded polypyrrole on microporous PDMS. Reproduced with permission.[70] Copyright 2019, Wiley-VCH.

the sensor. Tactile sensors based on a hierarchical porous structure of sensing materials were also developed to achieve linear sensitivity over a broad pressure range (2.53 kPa^{-1} with a detection range from 0.6 Pa to 200 kPa).[60] As shown in Figure 3b, the authors fabricated rGO-coated hierarchical foams via high-internal-phase emulsion polymerization, where small pores are packed between the larger pores. The hierarchical porous structure efficiently distributes stress and enhances deformation homogeneity, improving the detection threshold and operational range of the sensors. Besides structural modification of sensing materials, Jeong et al. reported that designing the geometry of the pressure-induced contact between two conducting electrodes can result in linear output signals over a wide pressure range.[62] The authors proposed a resistive-type pressure sensor, comprised a top electrode fabricated on a lenticular-structured polymer, and a patterned, planar bottom electrode (Figure 3c). The pressure-induced deformation of the lenticular structure changes the contact area between the top and bottom electrodes, forming electron-shortcut pathways along the designed circuit on the bottom electrode. By patterning the bottom electrode, the authors adjusted the induced electron-shortcut pathways, which demonstrates the tunable functionality of sensor parameters, such as detection range, linearity, and noise-band filtering.

Another approach for maintaining high sensitivity over a broad pressure range is to use multilayer geometry, which increases the change in the contact area and stress distribution to each layer.[23,58] Lee et al. reported a tactile sensor with high sensitivity (47.7 kPa^{-1}) over a wide pressure range (1.3 Pa to 353 kPa) by exploiting a multilayer, interlocked microdome geometry (Figure 3d).[58] A sharp increase in the contact area between the interlocked microdome arrays enhanced the sensitivity, while the increased changes in the contact area, and stress distribution between the stacked multilayers dramatically improved the linear operational range compared to sensors with monolayer designs. High sensitivity and linearity of the sensor facilitated the detection of various stimuli from low to high pressure, including weak gas flow and foot pressure. Pyo et al. also reported enhanced sensitivity and linearity of tactile sensors with multilayered designs.[23] The authors adopted hierarchical, porous structures of fabrics as a sensing material and stacked those into multilayers. The sensor with a three-layer structure exhibited enhanced sensitivity (26.13 kPa^{-1}) and linear range (0.2–982 kPa) than the single-layer device, which showed a sensitivity of 7.47 kPa^{-1} and a linear range of up to 100 kPa.

3.3. Response Time and Hysteresis

Response time determines the time for sensors to obtain a stable output signal in response to external stimuli (**Figure** 4a) and is crucial in real-time, dynamic applications such as pressure mapping displays, and instant user-interactive systems. For resistive and capacitive sensors based on polymeric materials, the viscoelasticity of polymers is the major cause of slow responses because of the time required for the deformation and recovery of the polymer chains. The use of non-polymeric materials, or structural designs that can reduce the deformation of polymer chains by creating additional free volume space, can address viscoelasticity and enhance the response speed of the sensor.[47,64–66] Several sensors with microstructures, such as pyramid[19] and porous structures,[25] and devices based on non-polymeric materials such as textiles[67] and tissue papers,[65] have been reported to achieve quick responses that are comparable to those of the human skin (≈15 ms).[1] Recently, tactile sensors with sub-millisecond responses were developed based on interlocked arrays of ITO nanospring structures.[68] Owing to the enhanced elasticity and self-recovery from the spring-like structures, the sensors could respond to a pressure of 10 kPa within 2 ms, and recover to the initial state in less than 1 ms (Figure 4b). With the sub-millisecond response times, the sensor was capable of measuring vibrating pressures ranging from 1 to 1000 Hz, with a signal-to-noise ratio of over 20 dB.

Hysteresis determines the inconsistency in the output signals when applying and releasing pressure (Figure 4c) and can be defined as the degree of hysteresis (DH) = $(A_{\text{loading}} - A_{\text{unloading}})/A_{\text{loading}} \times 100\%$, where A_{loading} and $A_{\text{unloading}}$ represent the areas of the loading and unloading curves, respectively.[69,70] The reduction of hysteresis is important for tactile-sensing applications because such differences in signals according to loading/unloading states result in measurement inaccuracy, and require additional circuitry and processing to compensate.[70] Hysteresis arises from diverse mechanisms such as the viscoelasticity of elastomers, weak interfacial adhesion between the conductive materials and polymer matrix, and the surface energy between the contacting elastomer surfaces. Resistive sensors based on conductive nanomaterials and elastomers, in which resistance varies through a change in internal conductive networks, particularly suffer from large hysteresis. This is because the conductive paths do not perfectly recover after deformation due to buckling of the conductive materials, or interfacial sliding between the nanomaterials and polymeric substrates.[71,72] Therefore, by designing materials and structures where resistance change does not rely on the deformation of the conductive networks among nanomaterials,[73] or by increasing the interfacial adhesion between materials and polymers to prevent the slipping or rearranging of materials, the hysteresis effect may be reduced.[74] Recently, Oh et al. reported tactile sensors with reduced hysteresis through chemically grafted polypyrrole (PPy) on a porous PDMS substrate (Figure 4d).[70] The strong chemical bonding between conductive PPy and PDMS reduced relative displacement, and change in the resistance was caused by the closing of pores in the materials rather than the relative movement of the polymer chains within the elastomer.

3.4. Spatial Resolution and Crosstalk

Tactile sensors with high spatial resolution have also been actively studied because these allow facile interfacing of complex tactile information, including object recognition and manipulation.[75] Various approaches, including structural designs of sensors and signal processing circuits, have been proposed to enhance the spatial resolution of tactile sensor arrays to be comparable to human touch, which can measure roughness with a resolution of 50 µm.[76–78] For high-density sensor arrays, the reduction in the interference of signals from adjacent cells, or crosstalk, is challenging. Crosstalk, which significantly diminishes the measurement accuracy, may occur from the mechanical load transmission to nearby, non-targeted cells, or from the leakage current through surrounding current paths.

Several studies have reported that the crosstalk effect can be reduced by the selection of appropriate materials, and sensor configuration. For example, to prevent response from adjacent, non-targeted cells, Pyo et al. added stiffer mechanical spacers between sensing cells (**Figure 5**a).[79] The sensors consist of a capacitor made of a PDMS/air dielectric between graphene electrodes and an SU-8 spacer. When pressure is applied, the dielectric layer of the sensing cells deforms, increasing the capacity between the two electrodes, while the SU-8 spacer prevents non-targeted cells from deforming. The authors demonstrated a 10 × 10 sensor array with 4.2 mm between sensing points with negligible cell-to-cell interference. Patterning sensing materials has also been proposed to mitigate the crosstalk effect by reducing leakage current.[73] Park and coworkers demonstrated resistive tactile sensors composed of a CNT-coated, porous PDMS as the sensing material, and the top and bottom electrode arrays to measure electrical signals. They designed grooves in the sensing elements, which shrink the unexpected current path between the adjacent electrode lines, preventing current leak through non-targeted cells (Figure 5b). Compared to the reference device without the groove, which showed an interference level of up to 92%, the proposed sensor showed a reduced interference level of 4%.

The integration of an active transistor matrix with sensors, or the formation of Schottky junctions, provides an effective route to reduce electrical crosstalk and give high on–off ratios, facilitating the discrimination of activated and inactivated adjacent cells.[80–85] Nela et al. introduced a 16 × 16 tactile sensor array with high spatial resolution (single pixel of 4 mm) that successfully eliminates crosstalk through the CNT active matrix.[80] The sensor array comprised a CNT-based thin-film transistor (TFT) and pressure-sensitive rubber (PSR). When pressure is applied, decreased resistance of the PSR leads to the on-state of the TFT, and when released, the increased resistance of the PSR makes the TFT switch off. Molybdenum disulfide (MoS_2)-based, flexible active-matrix tactile sensors in 8 × 8 arrays with an active area of 2.8 × 2.8 cm^2 were also developed (Figure 5c).[81] The sensor response is determined by the piezoresistivity of MoS_2 and channel (MoS_2/aluminum oxide) resistance of the integrated TFT, and the TFT integrated into each cell independently controls each pixel, efficiently decreasing crosstalk. You and coworkers demonstrated a high-resolution tactile sensor matrix (100 pixels cm^{-2}) based on Schottky junctions between poly(3,4-ethylenedioxythiophene):poly(styrenesulfonate)-coated microparticles and bottom electrode made of ZnO/polystyrene composites (Figure 5d).[82] Rectification through a Schottky diode junction prevents current leakage, and the authors also

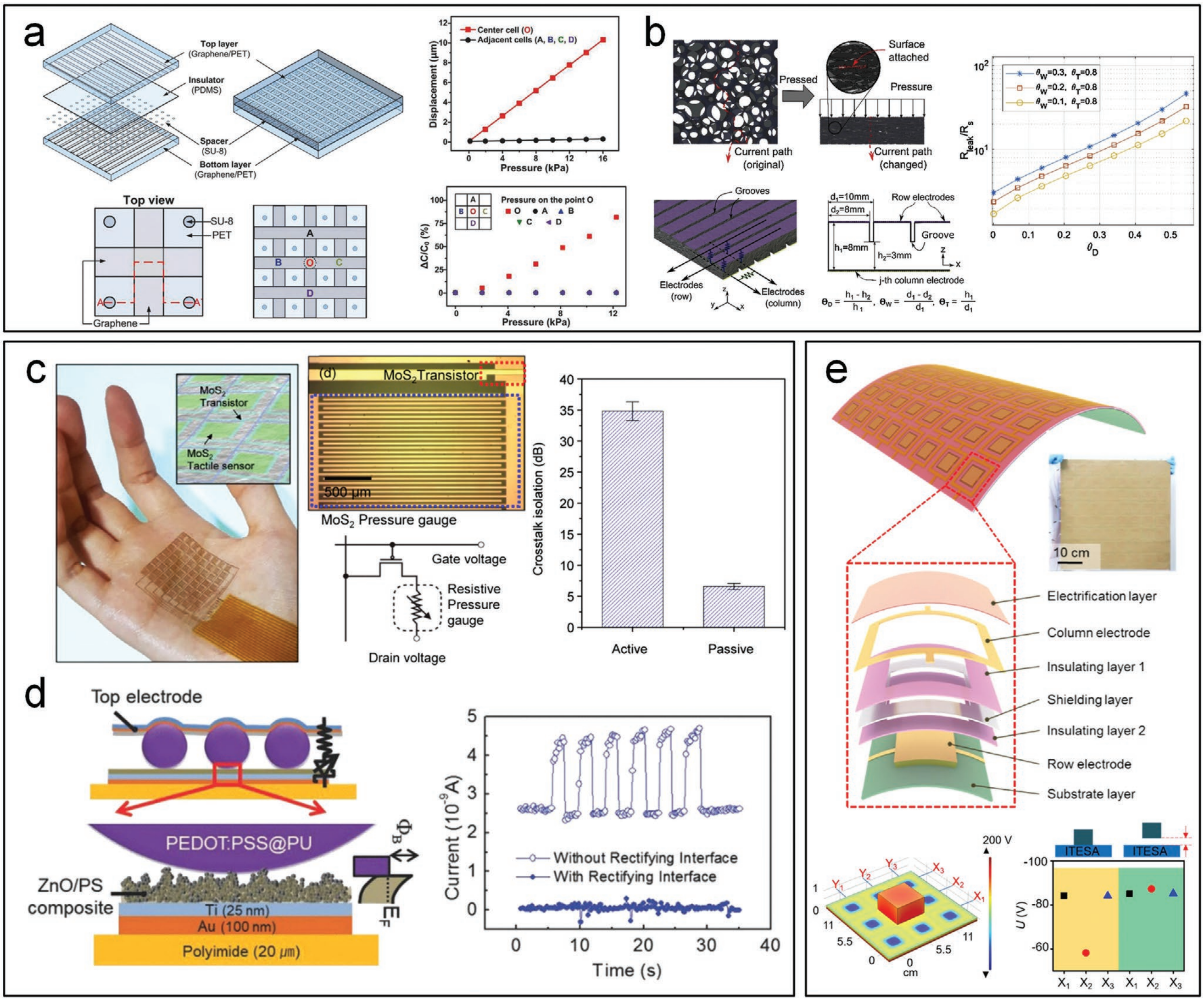

Figure 5. Strategies to prevent the crosstalk effect between adjacent cells. a) Crosstalk-free capacitive tactile sensors utilizing a rigid mechanical spacer. Reproduced with permission.[79] Copyright 2017, Wiley-VCH. b) Resistive tactile sensors with mechanical groove structures for interference reduction. Reproduced with permission.[73] Copyright 2019, Elsevier B.V. c) All-MoS_2 based, active-matrix-driven tactile sensor arrays exhibiting a reduction of crosstalk. Reproduced with permission.[81] Copyright 2019, American Chemical Society. d) Tactile sensor matrix based on a Schottky diode junction that reduces electrical crosstalk among pixels. Reproduced with permission.[82] Copyright 2018, Wiley-VCH. e) Triboelectric tactile sensor arrays with a low crosstalk effect based on the designated shielding layer. Reproduced with permission.[38] Copyright 2017, Elsevier Ltd.

addressed mechanical crosstalk using an ultrathin (1.4 µm) top electrode that prevents applied stress to the target cells from transmitted in the lateral direction through the electrode layer.

For triboelectric tactile sensor arrays, proper shielding has been reported to significantly reduce the crosstalk effect.[38,86,87] Adding an electrically grounded shielding layer between the electrodes, Zhu et al. designed an 8 × 8 triboelectric touch sensor array with electrification material made of PTFE textile and row and column electrodes (Figure 5e).[38] The shielding layer reduces interference between adjacent cells by preventing electrostatic induction between the electrode lines in the same layer and between the row and column electrode layers. Under external stimuli, target cells respond 100 times stronger than adjacent cells, allowing precise identification of an object's position. Conversely, without the shielding layer, the response difference between the neighboring and target cells is only 0.82 times because of the severe cell-to-cell interferences.

3.5. Multidirectional Force Detection

Apart from detecting the pressure applied in the normal direction, tactile sensors that can detect and differentiate multidirectional forces such as shear and torsion, are essential for interpreting complex contact information for texture, shape, and slip detection. In particular, it is imperative for physical interaction between humans and robots, such as robotic-assisted surgery and real-time force feedback systems.

Placing arrays of sensing elements, and simultaneously measuring the magnitude of multiple output signals, is one

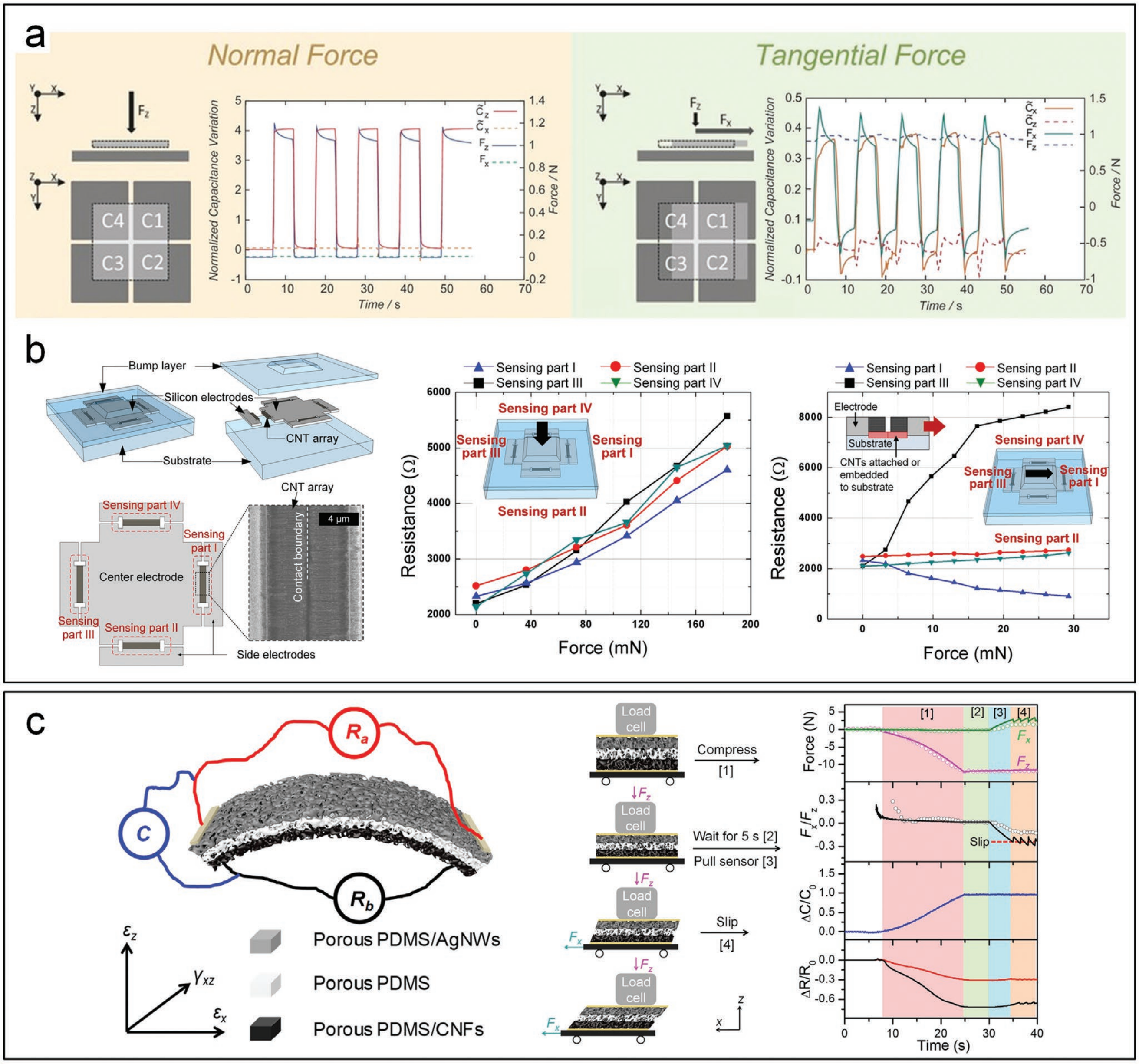

Figure 6. Approaches for multidirectional force detection. a) Capacitive and b) resistive tactile sensors capable of directional force detection by calibrating the responses of each sensing element. a) Reproduced with permission.[88] Copyright 2014, Wiley-VCH. b) Reproduced with permission.[90] Copyright 2018, IOP Publishing Ltd. c) Multidirectional sensor integrating resistive and capacitive responses to determine multiple forces simultaneously. Reproduced with permission.[92] Copyright 2020, American Chemical Society.

strategy for differentiating the direction of applied loads. For example, a capacitive sensor capable of discriminating 3D forces based on multiple capacitors has been demonstrated.[88] The sensor consists of four-unit capacitors, where four bottom electrodes share a common top electrode. Normal loads decrease the distance between the top and bottom electrodes, while shear loads vary the overlapping areas between them, changing the output capacitance of each element. By measuring and comparing the capacitance of the four sensing elements, the sensor could distinguish the direction of the applied force (**Figure 6**a). Triboelectric[89] and resistive sensors,[21,90] utilizing signals from arrays of electrodes, have also been proposed. As shown in Figure 6b, sensors based on four sets of facing CNTs differentiated the direction and magnitude of an applied force by measuring the resistance change according to the variation in the overlapped contact area between the CNT arrays.[90]

Utilizing two or more transduction mechanisms that respond to different mechanical loads is another method for multidirectional force sensing. Chen et al. developed sensors that can detect omnidirectional bending and normal force by combining resistance change and triboelectric voltage generation.[91] The sensors incorporate two CNT-PU conductive sponge strips intersecting each other as sensing materials, whose electrical resistance depends on the bending direction and curvature.

In addition, because the triboelectric voltage from the sponges only responds to normal pressure, the sensor can effectively differentiate the interference from external pressure. A multidirectional sensor based on resistive and capacitive signal transduction mechanisms was also developed.[92] This sensor consists of three stacked porous layers and a sandwiched dielectric layer between the top and bottom conductive layers. By measuring the changes in resistance of the two conductors and the capacitance between them, normal and shear loads, and slippage were simultaneously determined (Figure 6c).

3.6. Insensitivity to Mechanical and Environmental Conditions

With recent advances in micro/nanomanufacturing and materials technology, the flexibility of tactile sensors has rapidly improved, and their potential applicability has expanded. Wearable tactile sensors capable of being mounted on curvilinear and deformable human skin have advanced applications that were impossible with rigid tactile sensors, such as robot control by finger motion,[93] and e-skin.[37] For such applications, an ideal tactile sensor must exhibit stable sensing performance on human skin. However, mechanical deformation of the skin, such as bending, has a significant effect on pressure-sensing characteristics (variation in base signal[79] or sensitivity degradation under a bent state[94]) because most of the transduction mechanisms in tactile sensors are based on the change in electrical signal in response to mechanical deformation. In addition to the mechanical noise, ambient environment, such as humidity and temperature, also affects sensing characteristics. An increase in humidity level, for example, varies dielectric permittivity of the capacitive sensors and increases discharging of the induced charges in the triboelectric layer, impeding the accuracy and reliability of the measurements. To accurately detect pressure in human-interactive applications, the effect of bending and environmental conditions on the device performance should be minimized.

Recently, several groups have reported bending-insensitive tactile sensors.[18,27,95–97] One effective way to achieve bending insensitivity is to use a porous structure that can accommodate the bending-induced deformation. Lee et al. developed a nanofiber-based resistive pressure sensor that detects only the normal pressure, even under complex bending conditions (**Figure 7**a).[95] A nanofibrous material composed of elastomer, CNTs, and graphene was fabricated via electrospinning and functioned as a pressure-sensing material. When a strain is induced on the sensor by bending, the fibers are rotated and deflected instead of stretched, thus minimizing the strain applied to individual fibers. The relative alignment accommodates bending deformation, and therefore, the sensor maintained not only the base resistance, but also the sensitivity even under extreme bending conditions (a radius of curvature (ROC) of 80 µm). A wearable, bending-insensitive pressure sensor based on a CNT network-coated porous PDMS sponge (CCPPS) was also reported.[18] By conducting various experiments and numerical simulations, the authors verified that the porous morphologies of the CCPPS reduced the distortion of the CNT-coated PDMS bridges surrounding the pores under bent conditions, leading to no considerable change in the base resistance and sensitivity. Based on the bending-insensitive pressure-sensing capability and the ultrawide pressure-sensing range, a flexible foot insole for real-time detection of pressure distribution was demonstrated. Another approach to suppress the effect of bending on the sensor performance is to place the sensing part on a neutral plane that is not under compression or tension when bending is applied. Yoo and coworkers developed a transparent, bending-insensitive capacitive touch sensor via the percolation effect in a nanocomposite film.[27] In the sensor configuration, the sensing area was positioned near the neutral plane of the sensor, and the strain applied to the sensing area was only 0.4% at an ROC of 2.5 mm. Accordingly, the sensing performances of the sensor on curvilinear surfaces with an ROC ranging from 10 to 2.5 mm were similar (Figure 7b).

To reduce interference from humidity, several groups have utilized hydrophobic materials and waterproof encapsulation layers. Wang et al. demonstrated flexible and moisture-proof capacitive pressure sensors based on the hydrophobic poly(ionic liquid) nanofibrous membrane.[98] With the porous and hydrophobic dielectrics, the sensor exhibited stable, uniform responses under 30%, 50%, and 70% relative humidity condition, and even after repeated washings. Davoodi et al. reported improved humidity and chemical stability of resistive sensors when embedding conductive networks under the surface of the silicone.[99] The sensor had negligible humidity impact on sensing performance because the hydrophobic silicone surface prevented water molecules from reaching and interfering with the conductive network. The device also exhibited a longer shelf life, enhanced wash durability in the organic solvents such as isopropyl alcohol, ethanol, and acetone, compared to the reference device with a conductive network coated outer surface of the elastomer (Figure 7c). Diverse hydrophobic and waterproof coating/encapsulation layers, such as cellulose nanoparticles[100] and ethylene-vinyl acetate film[101] have also been utilized to protect triboelectric layers from environmental conditions.

Temperature also affects the resistivity and permittivity of materials and thereby sensing properties. However, screening the temperature effect completely with a single sensor is challenging, and several groups demonstrated decoupling temperature input by collecting and calibrating signals acquired in multimodal sensors. The details of multimodal sensors and decoupling of intermixed signals will be discussed in the next section.

4. Strategies for Integrated Tactile Sensor Systems

Besides the performance improvement of a single sensor, the integration with other components is important for practical applications. Ideal tactile sensor systems need to include multisensory capabilities to fully mimic human skin, power supply for operation, and signal processing. In this regard, various multimodal sensor systems capable of detecting various stimuli have been developed to provide enhanced functionalities beyond a single tactile sensor. Furthermore, a great deal of research has been conducted on self-powered sensor systems or the integration of sensors with flexible energy storage devices for realizing wireless, self-sustainable tactile systems. Recently, to enable signal processing and data transmission, the integration of sensors with wireless communication components has also been

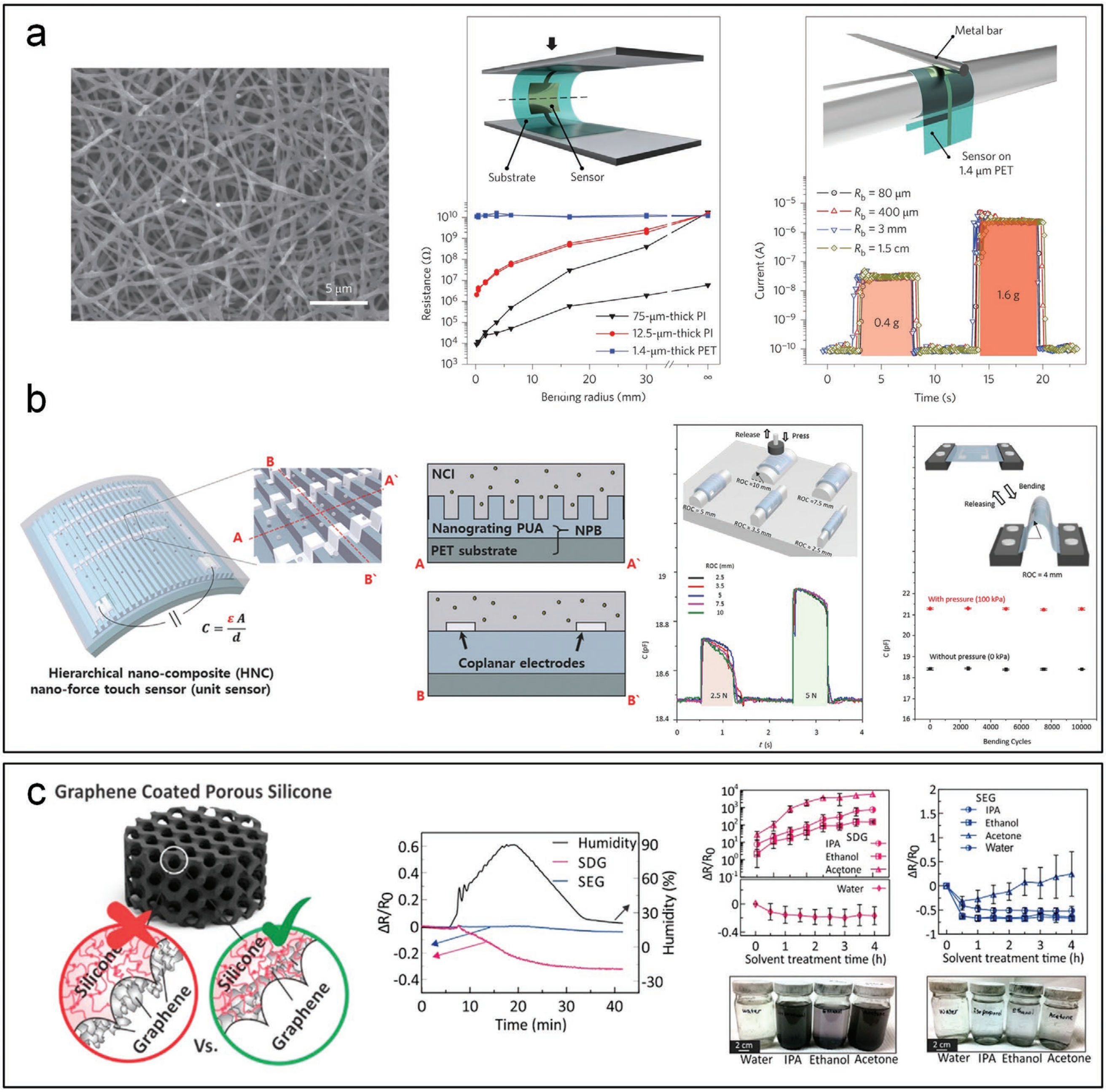

Figure 7. Novel materials and designs in tactile sensors for insensitivity to mechanical and environmental conditions. a,b) Bending-insensitive pressure sensor based on a) composite nanofibers of carbon nanotube and graphene and b) hierarchical nanocomposite. (a) Reproduced with permission.[95] Copyright 2016, Springer Nature. (b) Reproduced with permission.[27] Copyright 2018, Wiley-VCH. c) Designs to improve humidity and chemical resistance. Reproduced with permission.[99] Copyright 2020, American Chemical Society.

proposed. In this section, strategies for integrated tactile sensor systems including multimodal sensor systems, energy-autonomous systems, and wireless communication are described.

4.1. Multimodal Sensor Systems

Multisensory systems that can interface with complex human sensory systems to detect changes in the environment such as pressure, strain, temperature, and humidity, can provide enhanced interaction between humans and machines. For example, the ability to detect pressure and temperature is crucial for accurately identifying and safely manipulating objects.[102] Therefore, the development of tactile sensors capable of simultaneously measuring multiple mechanical and chemical stimuli has been actively investigated. Approaches for multimodal sensor systems can be divided into the utilization of single sensor modules responsive to

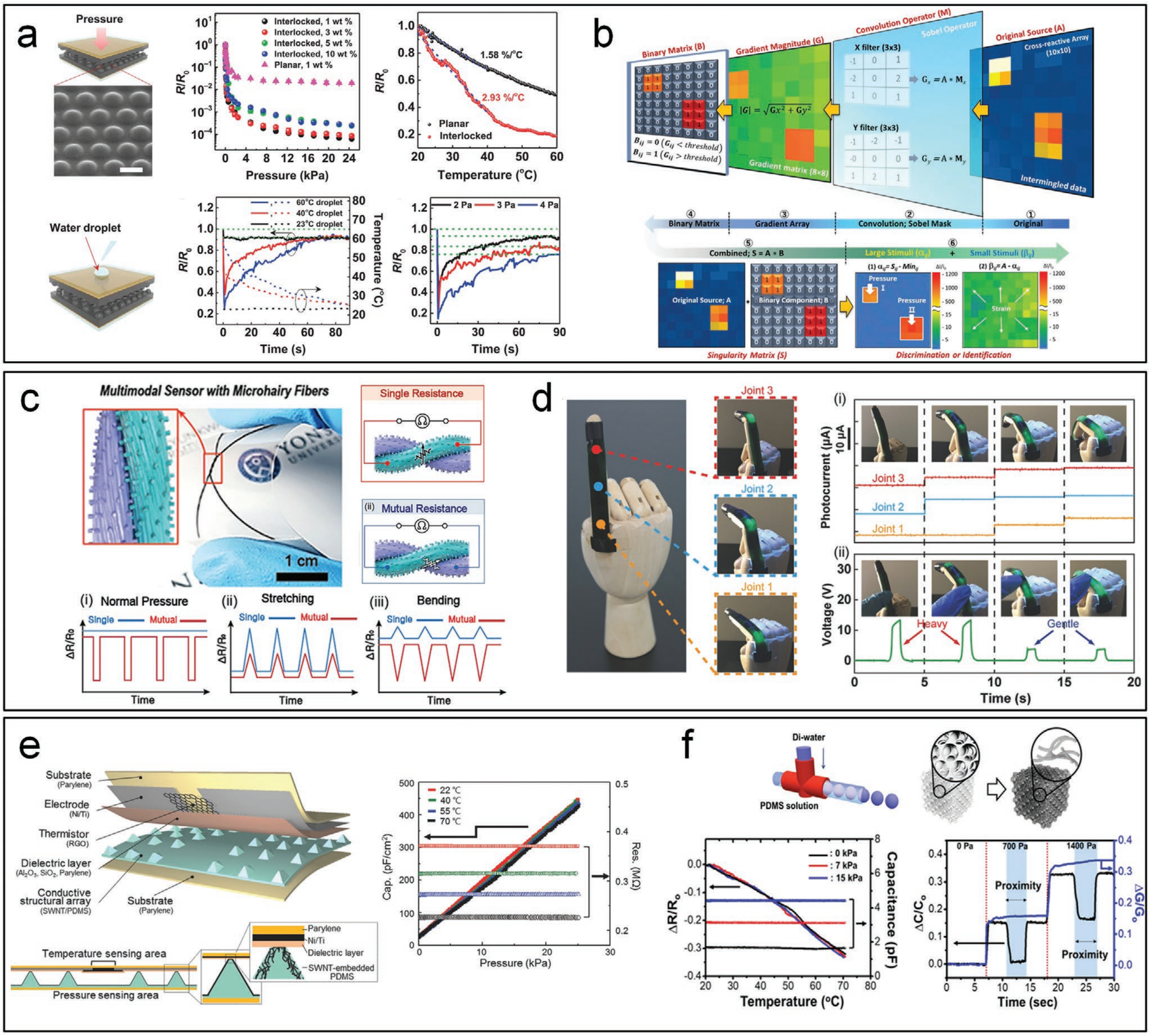

Figure 8. Multimodal sensor systems. a) Fingertip skin-inspired multifunctional sensors responsive to temperature and pressure. Reproduced with permission.[103] Copyright 2015, AAAS. b) Algorithm-based decoupling of mixed signals form multi-responsive sensors. Reproduced with permission.[16] Copyright 2020, Wiley-VCH. c) Multimodal sensors based on twisted, hierarchical conductive fibers that exhibit distinct waveforms of single and mutual resistance according to different external stimuli. Reproduced with permission.[109] Copyright 2019, Wiley-VCH. d) Stretchable triboelectric–photonic smart skin capable of simultaneous detection of lateral tensile and pressure via coupled photoluminescence and triboelectric effect. Reproduced with permission.[110] Copyright 2018, Wiley-VCH. e) Bimodal tactile sensor comprised pressure/temperature sensing elements that selectively respond to specific stimuli. Reproduced with permission.[102] Copyright 2018, Wiley-VCH. f) 3D microstructure-based sensing platform that can differentiate signals from pressure, temperature, and proximity. Reproduced with permission.[115] Copyright 2018, American Chemical Society.

multiple stimuli, and the integration of multiple sensors into a single platform.

As previously mentioned, one technique to achieve a multifunctional sensing system is to develop a single sensor that responds to multiple input stimuli. The simplest design includes sensors with a single transduction mechanism that exhibit different signal strengths depending on the type of input stimuli.[4,103–105] For example, Park et al. reported a tactile sensor with interlocked microdome array geometry, whose resistance varies according to applied pressure and temperature (**Figure 8**a).[103] These sensors are advantageous for simple device structures and measurement systems, but require additional processing for discerning intermingled signals. Decoupling of unknown input signals from such multi-responsive sensors was demonstrated by Tien et al.[106] The authors integrated piezo-pyroelectric gate dielectric and piezo-thermoresistive channel into the single field-effect transistor sensing platform, which responds to pressure and temperature simultaneously. By measuring the amplitude and offset values of the drain current under AC gate bias, a characteristic matrix that correlates the sensor responses to the amount of each applied pressure and temperature was derived, which was then used to estimate the unknown pressure and temperature values applied to the sensor. As recently demonstrated by Lee et al., applying a machine learning algorithm could also efficiently discriminate intermixed signals from pressure, strain, and temperature transduced via arrays of the resistive cross-reactive sensor (Figure 8b).[16] Therefore, further enhancement in sensor arrays with uniform sensing characteristics can provide an efficient route toward high-performance, multifunctional tactile sensors, with marginal complexity.

Devising a multi-responsive sensor and measuring signals from multiple outputs or transduction mechanisms render facile differentiation of mixed signals with relatively simple device configurations.[36,107–110] For instance, Park and coworkers demonstrated tactile sensors capable of differentiating normal pressure, strain, and bending by simultaneously measuring the resistance of the top and bottom electrodes and the capacitance between them.[36] Under normal pressure, capacitance between the electrodes increases with a negligible change in resistance of the electrodes. Under bending, both capacitance and resistance varied, but the change in resistance was only dependent on the bending and the lateral strain, and thus, the bending radius and direction and the lateral strain were detected by comparing the changes in the resistance of the two electrodes. Choi et al. developed twisted, conductive fiber-based sensors that can distinguish signals from the pressure, stretching, and bending of human gestures by discriminating waveforms of single-fiber resistance and mutual resistance between fibers in contact (Figure 8c).[109] Bu et al. demonstrated tactile sensors that detect strain and pressure via optical responses and triboelectric voltage generation, respectively (Figure 8d).[110] When strain is applied, designed microcracks appear in the metal film on top of aggregation-induced emission (AIE) compound, resulting in an increased photocurrent from the AIE. The sensor also works as a TENG-based pressure sensor, which shows a highly consistent response, regardless of the applied strain.

The integration of various sensors into a single platform is another approach for developing multimodal sensing interfaces.[26,111–114] Someya et al. demonstrated that laminating temperature-sensitive sensor networks on top of pressure-sensitive networks enables the simultaneous measurement of pressure and temperature distributions.[111] Hua et al. fabricated a flexible, multifunctional sensor matrix by integrating strain, temperature, humidity, pressure, magnetic, and proximity sensors.[112] In these devices, the reduction of interference from different stimuli is challenging because, in many cases, the sensing materials respond to several stimuli and generate coupled output signals. The careful selection of materials that make sensors respond to a specific type of stimuli is one promising method for discriminating signals. In this regard, a multifunctional sensor matrix responsive to humidity, temperature, and pressure has been developed by stacking an rGO-based temperature sensor and GO-based humidity sensor connected to graphene electrodes.[28] The resistance signals from rGO and GO and the capacitance between the graphene electrodes for pressure detection were not affected by the other two stimuli, thereby facilitating the distinction of mixed signals. Bae et al. also reported a multifunctional sensing platform that includes an rGO-based thermistor and capacitive pressure sensors (Figure 8e).[102] The resistance of the thermistor did not change with the amount of applied pressure, and the temperature-insensitive Al_2O_3 dielectric reduced the effect of temperature on pressure sensitivity. They also reported that the mixed output from temperature and pressure is easily discriminated using a single impedance analyzer owing to the linearity of both sensors. The combination of multiple sensors that can compensate for the responses of each other also enables the decoupling of mixed stimuli. For example, by combining a porous PDMS-based capacitive sensor with a porous PDMS/CNT-based resistive sensor, Kim et al. extracted the pressure, temperature, and proximity signals from mixed signals (Figure 8f).[115] Simultaneously applied temperature and pressure inputs can be distinguished because the capacitive sensor, which only depends on pressure, can calibrate signals from resistive sensors, which respond to both temperature and pressure. Similarly, the sensors can differentiate signals from pressure and proximity as resistive sensors, which are not affected by proximity, and can be a reference for decoupling the capacitance output from both.

4.2. Energy-Autonomous Systems

As tactile sensors integrated with a large density of sensors and electronic components have actively been developed, supplying stable, efficient power to such systems over a long time has become challenging. In addition to the high energy requirements, compact and flexible energy harvesting and storage devices that do not affect the portability and usability of the flexible systems are highly required.[116] As a way toward self-sustainable tactile systems, self-powered sensors that use collected power from external sources such as mechanical, thermal, and solar energy, have been extensively explored.

Piezoelectric generation is one of the widely used mechanisms for self-powered sensors. Various piezoelectric materials have been studied,[117,118] and advances in micro- and nanotechnology have enabled flexible piezoelectric nanogenerators with high power outputs and simple structures, which are highly applicable for tactile sensors.[31,32,119–121] Self-powered piezoelectric tactile sensors that can detect various human physiological signals were developed based on micropillar arrays of P(VDF-trifluoroethylene(TrFE))/barium titanate nanocomposites[120] and hierarchically interlocked PVDF/ZnO nanofibers (**Figure 9**a).[32] TENGs can also harvest various kinds of mechanical energy such as human movement[122,123] and vibration,[124] and have been widely adopted for self-powered sensor systems.[35] For example, 8×8 triboelectric sensor arrays based on a conductive fabric electrode and PTFE film generated sufficient power to modulate the on/off state of a connected complementary metal-oxide-semiconductor chip, enabling static pressure detection (Figure 9b).[87] Further integration with signal processing units allowed the sensor matrix to detect pressure and position, and to visualize the profile of contacting objects wirelessly.

Another sustainable energy source, thermal energy, can be harvested by using thermoelectric generators capable of converting a thermal gradient into electrical energy based on Seebeck effects or pyroelectric generators that collect energy

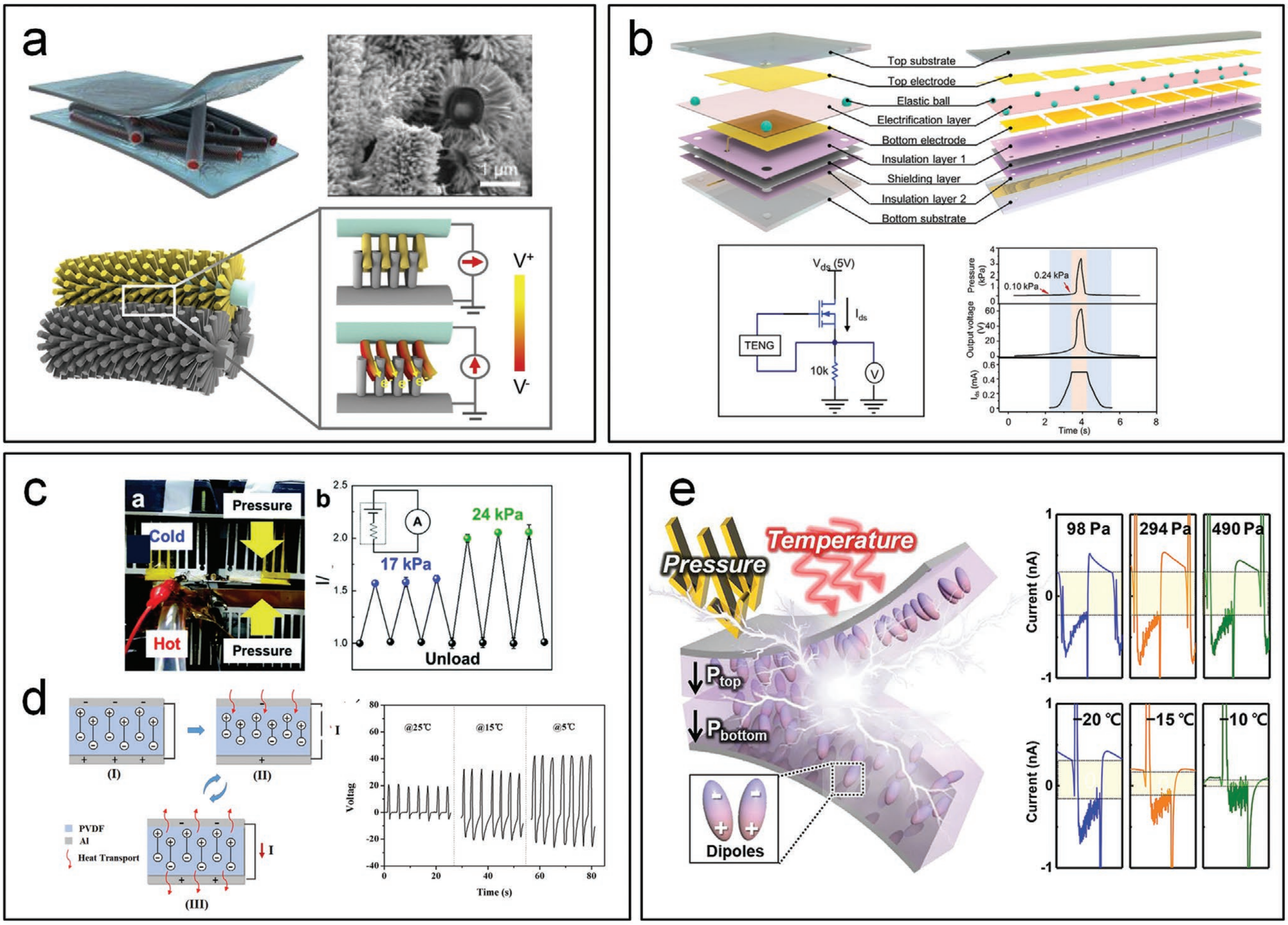

Figure 9. Self-powered tactile sensors for energy-autonomous systems. a) Self-powered tactile sensors based on a piezoelectric effect from hierarchically interlocked PVDF/ZnO nanofibers. Reproduced with permission.[32] Copyright 2020, Elsevier Ltd. b) Self-powered integrated pressure-sensor array based on the coupling of triboelectric sensors and CD4066 chip. Reproduced with permission.[87] Copyright 2019, Wiley-VCH. c) Self-powered pressure-sensor system composed of thermoelectric foams with piezo-resistive pressure sensitivity. Reproduced with permission.[128] Copyright 2018, The Royal Society of Chemistry. d) The working mechanism of the pyroelectric nanogenerators and their applications in self-powered breathing sensor. Reproduced with permission.[130] Copyright 2017, Elsevier Ltd. e) Self-powered, multimodal sensors based on polarization-tuned P(VDF-TrFE). Reproduced with permission.[134] Copyright 2020, Elsevier Ltd.

from the spontaneous polarization of dipoles because of time-dependent temperature variation.[125,126] Wearable thermoelectric and pyroelectric generators that obtain electrical energy from the temperature difference between the body and the environment have been actively explored, and self-powered wearable sensors based on these generators have been demonstrated.[127–130] Recently, Oh et al. developed compressible thermoelectric foams composed of poly(styrene-ethylene/butylene-styrene)-poly(3,4-ethylenedioxythiophene) polystyrene sulfonate that can work as thermoelectric energy harvesters as well as resistive pressure-sensing materials (Figure 9c).[128] The thermoelectric current from the materials at the same temperature gradient varies under different amounts of applied pressure, demonstrating the potential of a self-powered sensing system. Xue et al. reported pyroelectric nanogenerators based on PVDF and their application as self-powered breathing and temperature sensors (Figure 9d).[130] The authors also noted that pyroelectric generators can be a reliable energy source because they do not suffer from mechanical degradation.

In reality, multiple energy sources coexist in the environment, and sensors that simultaneously and individually collect these can enhance the reliability of the power supply. The integration of individual harvesting materials is one method for scavenging energy from multiple sources. Yang et al. developed flexible hybrid cells that can simultaneously and individually collect various energies.[131] In this work, thermal and mechanical energies are harvested by exploiting the pyroelectric and piezoelectric properties of flexible PVDF film, respectively, and solar energy is converted to electrical energy via the photovoltaic effect between a ZnO NW array and poly(3-hexylthiophene) film. Recently, Guo et al. reported self-powered e-skin based on the synchronized triboelectric effect from PDMS-AgNW film and the piezoelectric effect based on PVDF-TrFE nanofiber.[132] With these hybrid effects, the authors demonstrated a smart anti-counterfeiting signature system that can recognize writing habits such as pressure, velocity, and trajectory. Researchers also developed self-powered systems with multimodal sensing properties using materials that collect power from multiple

ADVANCED MATERIALS
www.advmat.de

energy sources.[133–135] For example, a self-powered sensor capable of pressure and temperature detection has been demonstrated by utilizing triboelectric and pyroelectric mechanisms from the polarity-modulation of ferroelectric P(VDF-TrFE) (Figure 9e).[134] More recently, barium titanate, which exhibits pyroelectric, piezoelectric, and ferroelectric photovoltaic effects, was also adopted to produce a self-powered, multimodal sensor system monitoring light, pressure, and temperature variations.[135]

For ideal energy-autonomous systems, the power needed for the entire system besides sensing components should also be considered. Therefore, flexible batteries or energy storage devices that store surplus energy for use in other components, for example, readout electronics, have also been actively investigated for continuous and reliable power supply to the entire system. The selection of materials and electrochemistry, with novel designs, has reduced the form factors and improved the efficiency of batteries and supercapacitors.[136–138] Photovoltaic cells are one promising energy devices owing to their high power-to-weight ratio and mechanical flexibility and robustness.[139] Núñez et al. reported that energy-autonomous tactile e-skin can be realized by heterogeneously integrating transparent tactile sensors on top of photovoltaic cells.[140] Further advances in flexible energy storage devices and integration with self-powered sensors can give additional reliability to energy-autonomous sensing platforms.

4.3. Wireless Communication

Measured data needs to be delivered and interpreted for practical applications. Wireless signal transmission is preferred, especially for wearable or implantable applications, due to the ease of communication and freedom of movement. Widely used technologies include electromagnetic coupling and Bluetooth communication. Electromagnetic coupling occurs between internal LC or RLC resonators—a series connection of inductor, capacitor, and resistor—and external resonators connected to readout systems. An applied stimulus changes the effective inductance[141,142] or capacitance[143,144] of the internal resonators, shifting resonant frequency (f) defined as Equation (1).

$$f = \frac{1}{2\pi\sqrt{L_e C_e}} \tag{1}$$

where L_e and C_e represent the effective inductance and capacitance of the internal resonators, respectively. The shift of the resonant frequency of internal circuits resulting from external stimuli can be detected by measuring the shift or the magnitude of the reflection coefficient (S11) via an analyzer connected to the electromagnetically coupled readout circuit.[145–147] Owing to the simplified electric connection and ease of miniaturization, electromagnetic coupling has been widely used in diverse wireless sensing applications.[143,145,148–150] For example, textile-based wireless pressure-sensor arrays were developed for remote human-interactive sensing.[142] As shown in **Figure 10**a, the device includes a fabric spacer, stacked between an LC antenna and ferrite film. Applied pressure deforms the fabric spacer, decreasing the distance between the antenna and ferrite films, which results in a resonant frequency shift of the LC antennas. The sensors could be attached to a flexible wrist band, insole of footwear, or a waistband, demonstrating diverse remote applications, for example, recording fingertip pressure, monitoring plantar pressure distribution, and measuring the interactive pressure between the belt and the abdomen. Recently, Lee et al. proposed wireless pressure sensors capable of simultaneous detection and discrimination of signals from multiple sensors in parallel.[143] The authors demonstrated pressure sensors based on PPy-coated PDMS pyramids connected to inductive coils with a specific number of turns, and three vertically integrated wireless sensor modules with antennas stacked on top of each other. (Figure 10b) An applied pressure decreases the magnitude of the reflection coefficients (S11) with a negligible frequency shift, and inductive coils with different numbers of turns assign distinct resonant frequencies of the reflection coefficient (S11) spectrum to each sensing element, facilitating signal differentiation.

When designing wireless devices based on electromagnetic coupling, several factors, such as frequency range, Quality factors (Q-factors), and efficiency, should be carefully considered.[151] The design of antennas that comply mechanically with target surfaces is also critical because mechanical deformation in the antenna structure can affect the resonant frequency and the Q-factors, resulting in performance degradation of the signal transmission.[147,151] Researchers have demonstrated antennas made with novel materials such as textile,[142] liquid metal,[152] and conductive nanomaterial-based composites[153] to enhance flexibility and stretchability. Structural engineering, including the serpentine[147] and 3-D configurations,[154] has also been applied for the stable operation of antennas under mechanical loads. For detailed requirements and designs of flexible and stretchable antennas, the reader is referred to Xie et al.[151]

Bluetooth is another widely used wireless communication module that can transmit signals over long distances. Several groups have reported Bluetooth-integrated sensor systems capable of interacting with processing units.[17,155–158] Zhong et al. demonstrated a wireless, wearable pressure sensor capable of monitoring human muscle activity by connecting sensors in series with a Bluetooth transmitter module and a battery.[17] The signals from wrist motions during daily activities, such as typing on a keyboard and opening a door with keys, could efficiently be transmitted to a mobile phone, exhibiting potential real-time human–machine interfaces and smart robotics (Figure 10c). Wu et al. introduced a wireless gait-monitoring system by connecting pressure sensors fabricated on a soft shoe insole with a Bluetooth module.[159] Signals acquired from sensors on different positions of the shoe pad were converted, processed, and transmitted to receivers via Bluetooth, realizing instantaneous mapping of the plantar pressure data during walking. Using miniaturized Bluetooth modules mounted on flexible printed circuit boards (FPCBs) can further enhance the flexibility and wearability of Bluetooth-integrated wireless sensing platforms.[160,161] As shown in Figure 10d, Gao et al. developed fully integrated, wearable sensor arrays capable of transducing signals from temperature and chemicals on human skin via multiplexed sensor arrays, processing data through the integrated circuit on the FPCB, and transmitting data to a mobile phone using Bluetooth.[160]

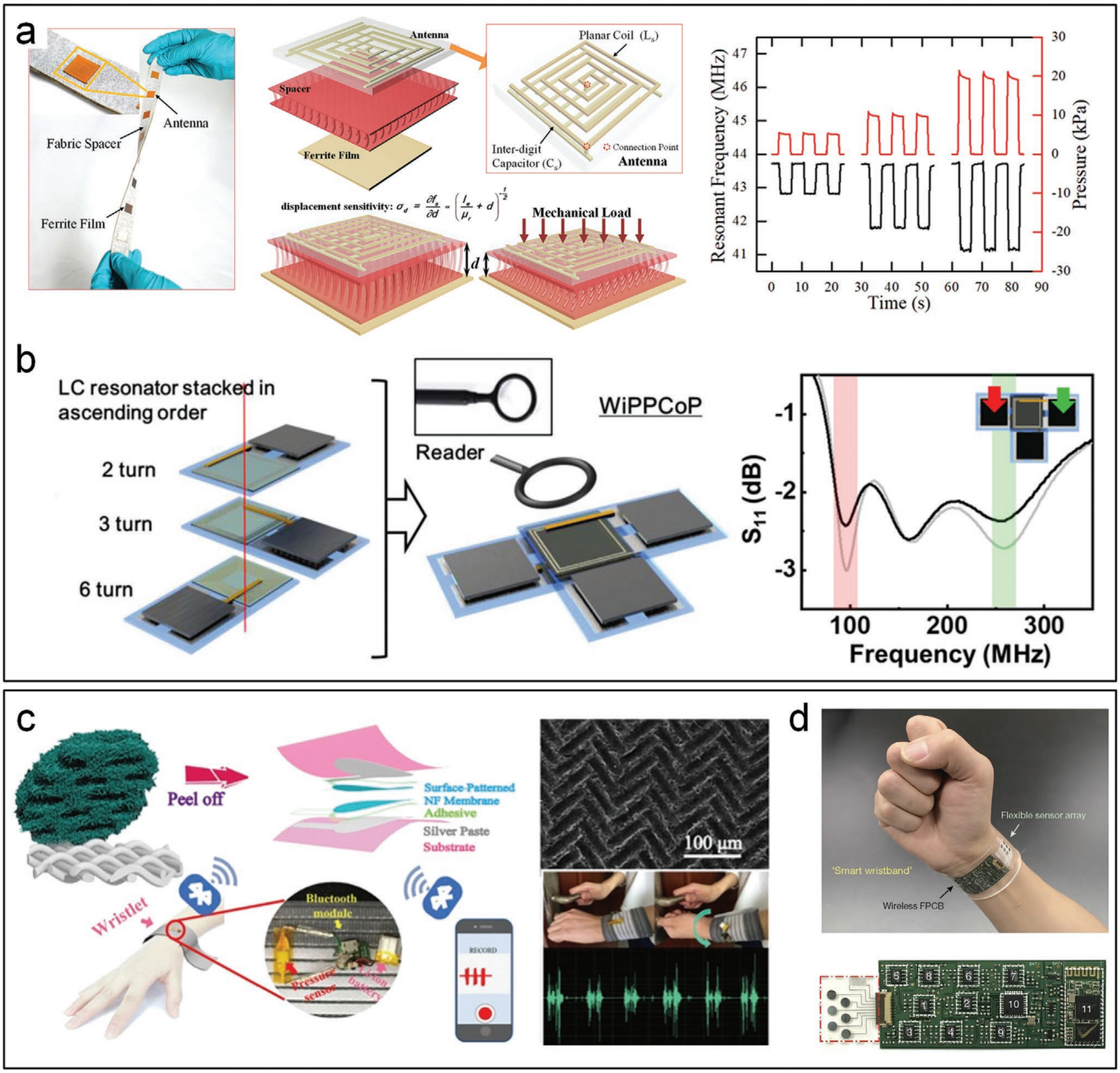

Figure 10. Wireless communication for wearable applications. a) Textile-based wireless pressure sensors based on a fabric spacer sandwiched between passive antennas and ferrite films. Reproduced with permission.[142] Copyright 2019, Wiley-VCH. b) A wireless pressure-sensing platform capable of simultaneous processing of signals from multiple sensors. Reproduced with permission.[143] Copyright 2019, Wiley-VCH. c) Wearable pressure sensors with a Bluetooth module for wireless human-motion monitoring. Reproduced with permission.[17] Copyright 2018, American Chemical Society. d) Fully integrated wearable sensor arrays combined with multiplexed sensors, integrated circuits for signal processing, and a Bluetooth module for signal transmission. Reproduced with permission.[160] Copyright 2016, Springer Nature.

5. Integrated Tactile Sensors for Human-Interactive Systems

5.1. Artificial Electronic Skin

Artificial skin for robots and prostheses that mimic the tactile sensitivity of human skin are crucial applications for tactile sensors. Robots equipped with a tactile sensor and feedback system enable more delicate and complicated functions, such as gripping and manipulating fragile objects, or detecting properties of materials, than those relying only on visual perception.[162] Furthermore, the addition of skin-like sensing properties to prosthetics can provide an opportunity for patients with missing limbs or damaged skin to restore sensing capabilities, which plays a critical role when interacting with their environment.[1,163] Therefore, there has been considerable interest for the development of multifunctional, flexible tactile-sensing platforms for robots or prostheses to

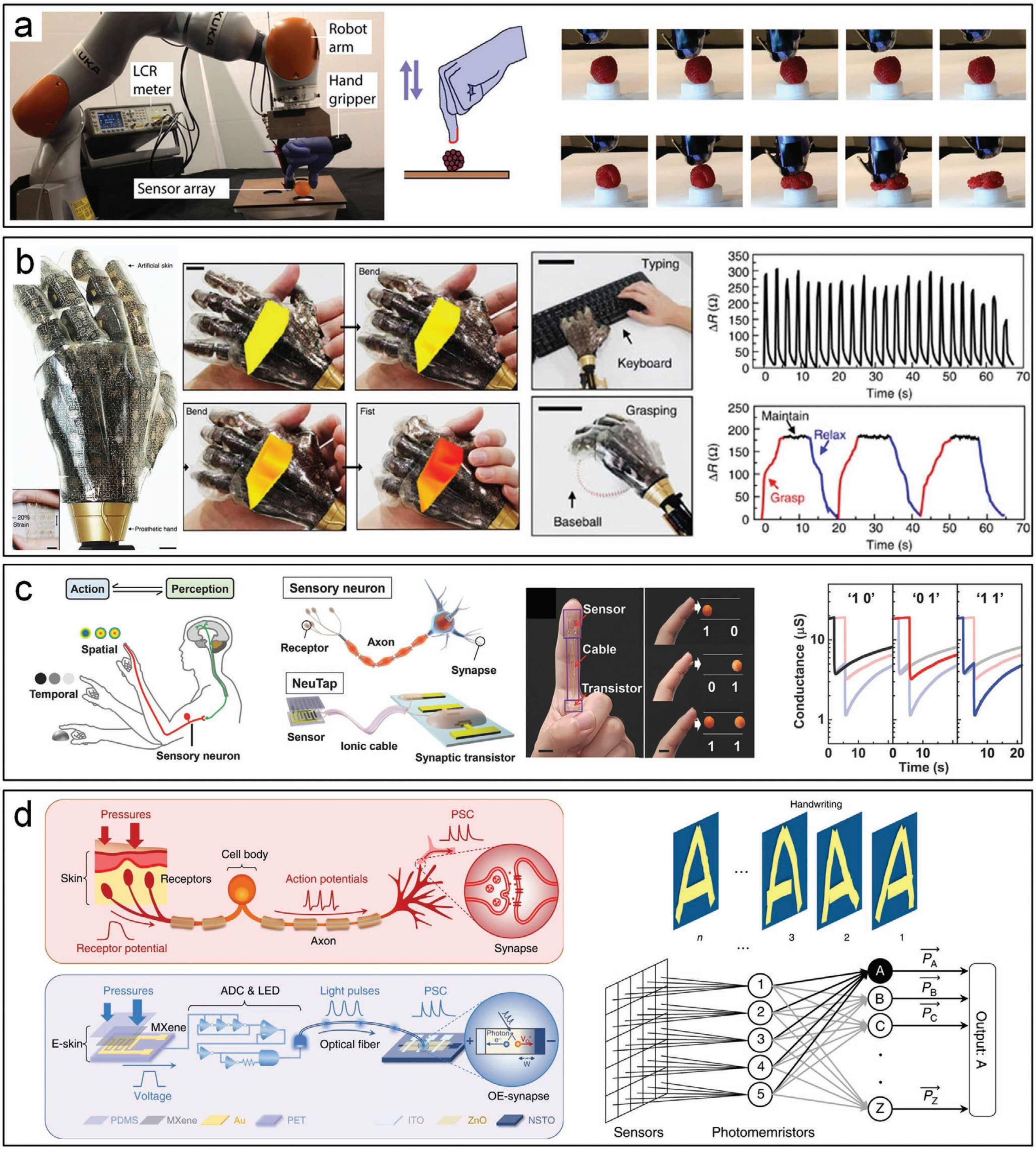

Figure 11. Artificial electronic skins for robotic and prosthetic applications. a) Robotic gripper equipped with closed-loop tactile feedback capable of interacting with fragile objects. Reproduced with permission.[165] Copyright 2018, AAAS. b) Artificial skin for a prosthetic limb that responds to daily life situations. Reproduced with permission.[169] Copyright 2014, Springer Nature. c) Artificial sensory neuron that mimics human perceptual learning. Reproduced with permission.[172] Copyright 2018, Wiley-VCH. d) Bioinspired, artificial optoelectronic afferent nerve systems that can recognize and learn handwritten words. Reproduced with permission.[175] Copyright 2020, Springer Nature.

enable human-like dexterity. With novel materials and technological advances in sensors, signal processing, and transmission, several groups have reported artificial sensory skin for robotic and prosthetic applications.[164–168] As shown in **Figure 11**a, Boutry et al. demonstrated a dexterous robotic hand with tactile sensing and feedback capability by utilizing soft e-skins capable of real-time measurement and discrimination of normal and shear forces.[165] The e-skin comprised facing CNT/PU composites with designed surfaces mounted on an artificial hand. The signals from normal and tangential forces were recorded by an LCR meter and retrieved by the robotic controller to program the next movement of the arm. Compared to the reference model without tactile feedback, the robotic arm with a closed-loop control system could interact with fragile objects (e.g., raspberries) without crushing them. Oh et al. reported a soft robotic hand with multiple sensors and wireless electronic circuits.[166] Si transistor-based pressure and temperature sensors were mounted on the finger-like soft actuators consisting of a silicone elastomer mixed with ethanol and liquid metal microcapsules. Wireless actuation of robots, as well as real-time monitoring of tactile pressure and temperature through a mobile phone, was successfully demonstrated by connecting the robot with electronic circuits, including a microcontroller unit, Bluetooth module, and signal amplifier. Kim et al. demonstrated a multifunctional e-skin-based prosthetic hand that responds to various daily life situations.[169] The e-skin could detect diverse stimuli such as pressure, temperature, strain, and humidity, and deal with complex situations (Figure 11b). Strain sensors monitored minor movements near the fingers and joints during handshaking, and pressure sensors reliably transduced signals from typing and grasping an object. The temperature and humidity sensors also provided feedback when the prosthetic hand held a hot or cold drink or touched dry or wet surfaces. Furthermore, the authors demonstrated that input signals from pressure sensors were successfully transferred to the nervous system by connecting pressure sensors with the nervous system. Further development in tactile-sensing platforms, combined with advanced neural interface technologies,[170] may allow amputees to achieve tactile sensitivity comparable to, or even better than, human skin.

In addition to the transduction of input signals, efforts have been made to develop artificial nervous system that mimic biological signal processing and learning behavior.[171–177] In biological systems, external stimuli perceived by sensory neurons induce action potential, which is then transferred by nerve fibers and combined through synapses before being processed.[175,178] To implement similar functionality, artificial nerves, which comprised sensors to receive tactile stimuli, electronic circuits to encode and transmit the signals, and synaptic transistors to process the input data for learning and recognition, have been demonstrated. For example, Wan et al. reported an artificial sensory neuron constructed of CNT/PDMS-based resistive pressure sensors, ionic cable, and a synaptic transistor that can learn and recognize input patterns, mimicking the function of tactile perceptual learning (Figure 11c).[172] Tan et al. connected pressure sensors to an analog-to-digital converter and a light-emitting diode circuit, through which the tactile signals were encoded to light pulses,[175] which were then transmitted to postsynaptic circuits. With a neural network learning algorithm, the artificial nerve system recognized, learned, and memorized words handwritten on the sensors (Figure 11d). As with the extensive amount of data required to be processed rapidly and energy-efficiently, computing efficiency has been getting more and more attention. For details of advances in computation with tactile sensors, the reader is referred to Dahiya et al. [116,179] Combined with efficient memory and computing technologies, biomimetic systems for tactile sensory coding and learning provide a promising strategy for mimicking the cognitive functions of humans, which can pave the way for robots and amputees to achieve dexterity comparable to the human hand.

5.2. Control Interfaces

Flexible tactile sensors have also been widely developed to provide novel types of interfaces between humans and machines. Conventional input devices or control interfaces are based on rigid sensors or actuators that limit conformal, seamless interfacing due to user discomfort from the mechanical mismatch between the human skin and the instruments. Owing to their mechanical compliance with the human body, wearable tactile-sensing systems are expected to introduce new communication methods between humans and ambient electronics with real-time, high-speed interactions.

Various designs for flexible tactile sensors that interface with machines have been proposed, including smart gloves,[96,109,180] keyboards,[40] and touch panels.[27,181,182] Choi et al. demonstrated a smart glove by integrating fiber-based tactile sensors.[109] The glove can distinguish the strain, pressure, and bending of fingers by monitoring the single and mutual resistance of twisted fibers. The authors then developed a program that converts signals from the gloves to be used as a control interface for virtual shooting games (**Figure 12**a). Dong et al. also developed a self-powered tactile-sensing glove capable of real-time robotic control and VR/AR communication.[183] The TENG-based sensors are connected to a nanophotonic readout circuit composed of aluminum nitride and a Mach–Zehnder interferometer modulator that transduces triboelectric signals to photonics, suppressing electrical state shifts. The stable, real-time photonic signal enabled the wireless control of a toy car driving on a road and a drone in VR. Moreover, the authors demonstrated the control of a robotic hand that responds to signals transduced in sensors on each finger of a glove, and the motion control of hands in AR to plant flowers (Figure 12b). Huang et al. demonstrated a universal interactive system based on flexible tactile sensors with diverse materials and configurations.[40] The device combines TENG-based tactile sensors on textiles and papers with an optical communicator and a microcontroller unit (MCU). External stimuli such as touch, press, and contact, induce triboelectric signals, which then operate LEDs that modulate a photoresistor connected to the MCU. Such conversion transforms messy current signals from TENG into standard digital signals for object control such as the management of a software program and the modulation of the brightness of a desk lamp (Figure 12c). In addition, hands-free interfaces that can expand the way people interact with electronic devices have been developed. Tactile sensors mounted on eyewear, for example, enabled signal acquisition from blinking, which can be processed to control daily electrical appliances[184] or monitor driver behavior.[185]

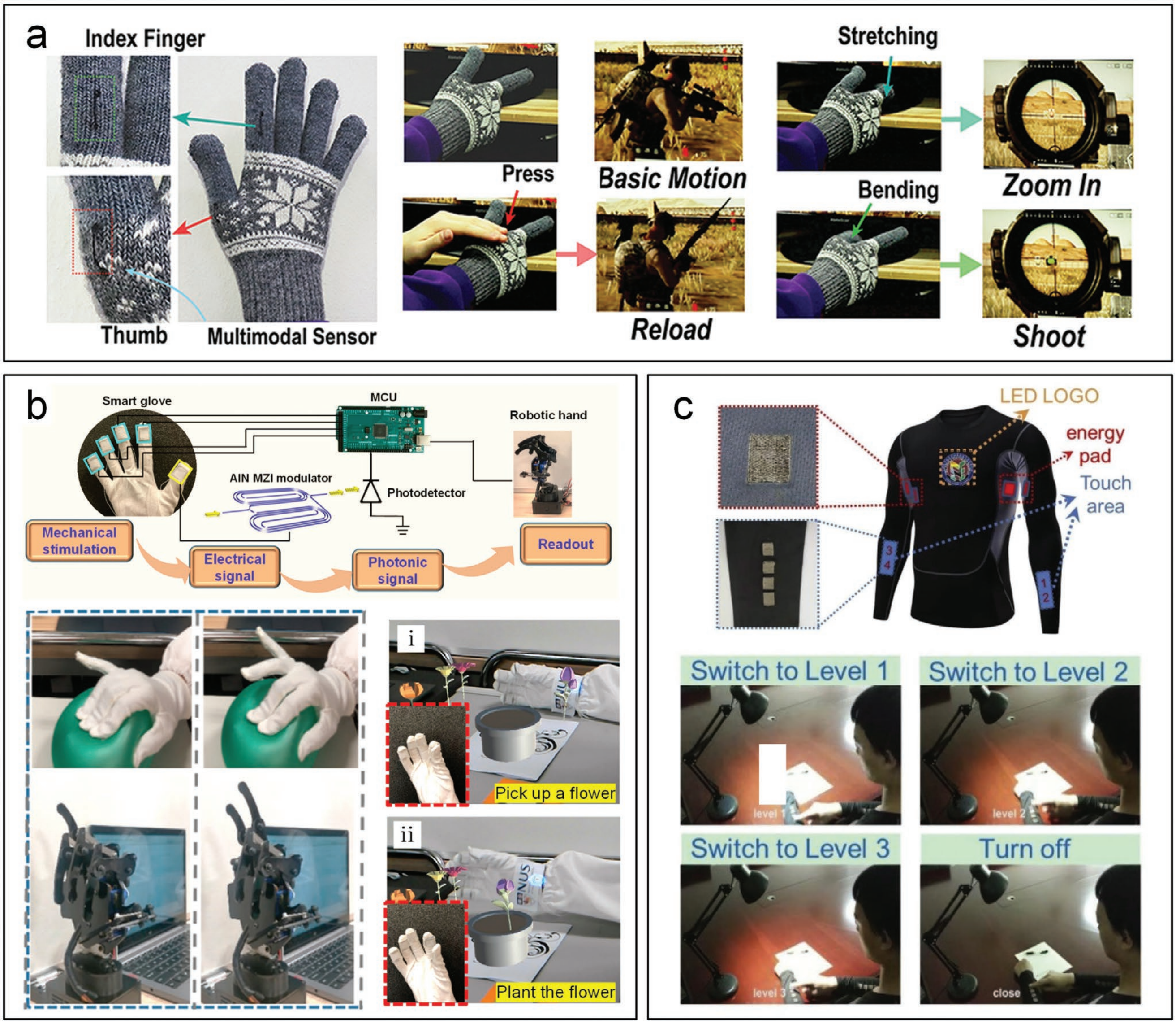

Figure 12. Tactile sensor-based control interfaces. a) Wearable tactile-sensing gloves for pressure and gesture-discernible gaming control interface. Reproduced with permission.[109] Copyright 2019, Wiley-VCH. b) Smart glove for real-time robotic hand control and VR/AR interaction. Reproduced with permission.[183] Copyright 2020, American Chemical Society. c) Textile-based wearable tactile interactive system that can wirelessly control target devices. Reproduced with permission.[40] Copyright 2019, Elsevier Ltd.

5.3. Interactive Tactile Interfaces

Interactive human–machine interfaces that give feedback from machines to the users have also attracted significant attention because these can complement visual and auditory information, and bridge humans with VR or AR. Widely used technologies for feedback actuation include an electrotactile display that evokes the skin sensation by transmitting current through electrodes, and a mechano-tactile display that induces responses of mechanoreceptors via mechanical stimulation.[186] Several bidirectional interfaces have been realized by connecting tactile sensors and displays. Lim et al. reported an interactive human–machine interface based on wearable sensors and actuators (**Figure 13**a).[8] The epidermal piezoelectric motion sensors, consisting of nanomaterials and piezoelectric polymer (polylactic acid), detect signals from bending, relaxing, and pressing a human wrist, and the signals are converted to control the robot. When another piezoelectric sensor on the robot arm detects the gripping of an object, the electrotactile stimulator attached to the forearm is activated, providing electrical feedback to alert the user. Zhu et al. developed a haptic-feedback system for VR and AR applications.[9] Through triboelectric finger and palm sensors, multidirectional mechanical inputs such as bending fingers, and sliding palms, were monitored and delivered to virtual spaces, and the converse piezoelectric effect from a piezoelectric haptic stimulator generated vibration feedback to users (Figure 13b). The authors demonstrated the application of such interfaces in virtual baseball gaming, whereby

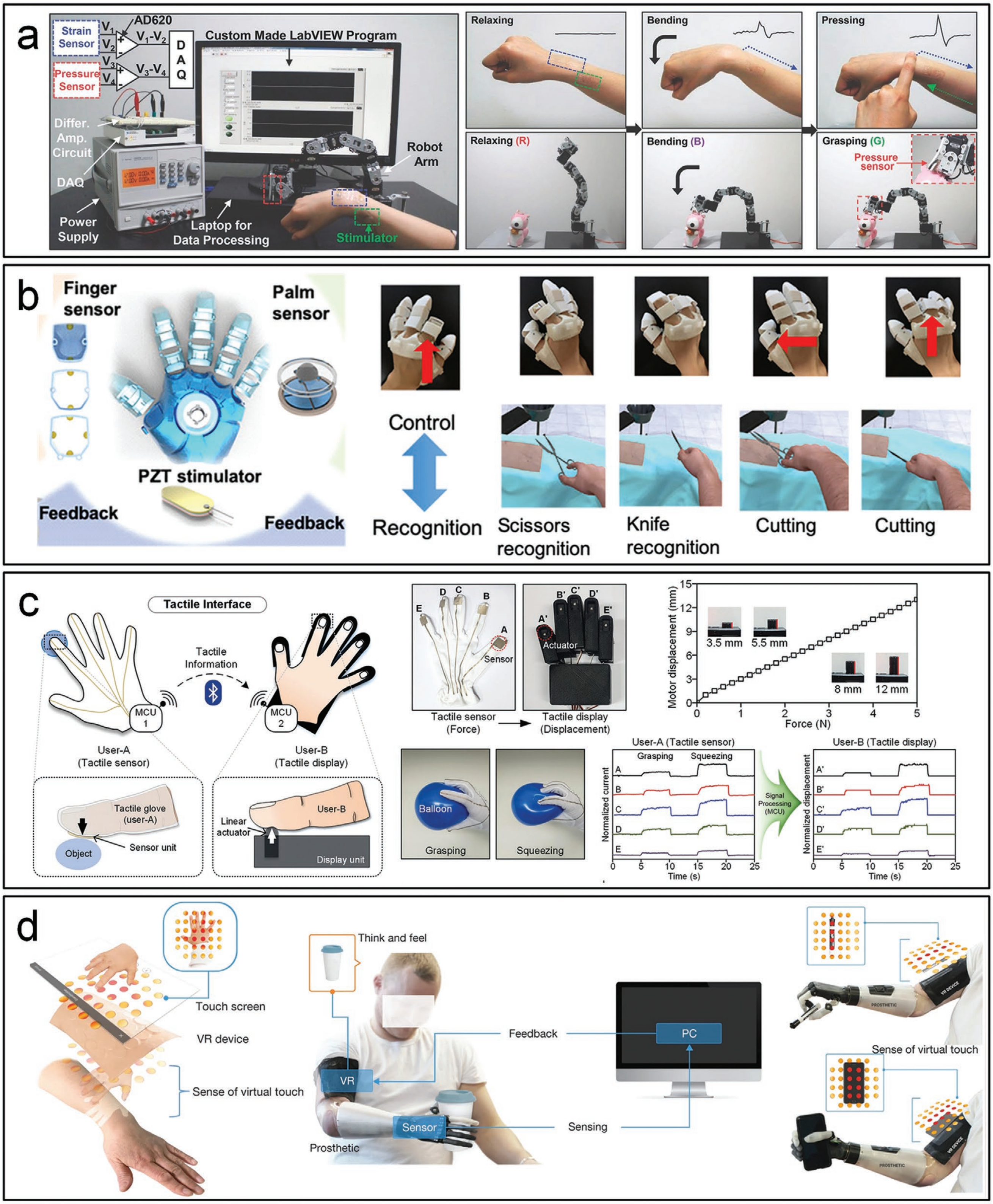

Figure 13. Bidirectional tactile interfaces. a) Interactive human-robot interface based on piezoelectric motion sensor and electrotactile actuator. Reproduced with permission.[8] Copyright 2014, Wiley-VCH. b) Haptic-feedback smart glove for interactive human–machine interface and VR/AR applications.[9] Copyright 2020, AAAS. c) Textile-based wearable tactile interface that can transmit the tactile information to a distant user. Reproduced with permission.[23] Copyright 2019, Wiley-VCH. d) Epidermal wireless haptic interfaces for prosthetics and VR/AR applications. Reproduced with permission.[187] Copyright 2019, Springer Nature.

sensors translated swinging actions into a VR environment, and PZT actuators fed information about the virtual collision of the ball back to the user. Leveraged with machine learning algorithms, the interfaces could perform intuitive jobs, for example, object recognition and VR surgical training. Wireless tactile interfaces, through which the tactile information can be delivered to a distant user, were also demonstrated.[23] Pyo et al. devised an interface consisting of fabric-based pressure sensors attached to cotton gloves, a linear-actuator-based mechanotactile display, and two MCUs for Bluetooth communication. As shown in Figure 13c, the touch information sensed by user A wearing gloves with sensors on each fingertip is processed and transmitted to the tactile display via Bluetooth. Simultaneously, linear actuators corresponding to individual sensors are activated, allowing user B to sense the transferred information by laying his or her hand on the display. Based on careful material selection and geometric design, Yu et al. advanced wearable haptic displays with wirelessly controlled and powered vibratory actuators (Figure 13d).[187] The vibratory actuators, consisting of a Cu coil and permanent magnet, were connected to near-field communication antennas and integrated circuits for wireless operation and individual control. Using this skin-mountable haptic interface, the authors demonstrated a variety of applications, including the tactile feedback of prosthetics, delivery of virtual tactile touch to distant users, and reproduction of the impact on game characters to users. Further advances in tactile display technology toward multiplexed feedback sensation may broaden the spectrum of applications, for example, remote medical practice, remote exploration, VR, AR, and multimedia entertainment.

6. Conclusion and Outlook

Flexible tactile sensors have been actively studied due to their diverse applications. There has been considerable development of tactile sensors based on advances in the fields of novel materials and micro/nanoengineering. In this review, we have summarized recent progress in flexible tactile sensors, ranging from designs to advance sensing performance, to endeavors made to realize integrated devices and their applications in human-interactive systems. We have briefly outlined representative sensing mechanisms such as resistive, capacitive, piezoelectric, and triboelectricity, and highlighted materials and design configurations attributed to enhanced sensing properties. These included sensitivity, detection range and linearity, hysteresis and response time, spatial resolution, multidirectional detection, and insensitivity to mechanical and environmental conditions. For a specific parameter, many tactile sensors with high-performance comparable to or better than human skin have been developed. These sensors with improved capabilities, such as enhanced sensitivity, broader sensing range, or faster response time surpass human skin, providing new applications. However, the development of tactile sensors that address all of the properties of human skin remains a significant challenge. For example, the sensor based on bristled microparticles could distinguish extremely small force (≈3 μN) and exhibited fast response time (≈7 ms), but high sensitivity and linearity maintained only in the low-pressure region (<20 Pa).[54] Achieving the skin's spatial resolution without crosstalk and performance uniformity between tactile cells is also challenging due to technological and manufacturing issues. Accordingly, it is important to prioritize performance metrics according to the application to determine which design and material configurations are appropriate. We believe this review will serve as a useful reference for researchers interested in improving the performance of a tactile sensor. We have also reported tactile-sensing systems with improved integration density that enabled multifunctional sensing and feedback systems hybridized with energy devices and wireless communication modules. These mechanically flexible, wireless, and energy-autonomous systems provide promising ways of communication that can expand the interaction between human and electronic devices. We have highlighted applications of tactile-sensing systems in artificial e-skin for robotics and prosthetics, wearable controller for electronic devices, and bi-directional communication tools between distant users and the VR/AR environment.

In future research, several factors require further consideration. 1) In addition to mechanical flexibility, tactile sensors should not block the physiological activity of the skin or organs. For example, although mechanically compatible, flexible sensors that interfere with sweating or breathing of the skin are not suitable for continuous, long-term applications because they can cause damage. Therefore, high-performance tactile systems with advanced functionality, for example, biocompatibility and biodegradability, should be investigated. 2) The environmental stability of the systems needs to be categorized and examined. The measurement of the working reliability of the devices has been focused on operation under repeated mechanical strain or pressure. However, environmental factors that the devices encounter in daily activities such as humidity, sweat, and water permeation, can also be significant causes of performance degradation in long-term usage, and therefore, the chemical and environmental reliability of human-interactive systems, as well as biocompatible encapsulation technology, should be further considered in designing the systems. 3) A high-level, large-area integrated device platform with cost-effective, scalable fabrication methods should be investigated for the industrialization and real-life applications of a fully integrated sensing platform. 4) Research on tactile sensors and the human-interactive systems should be coupled with advances in signal processing and computation. Extracting meaningful data from noisy, mixed signals from daily activities in real time is critical for practical uses, including accurate detection of motions, biological signals, and instant VR/AR communication.

Acknowledgements

S.P. and J.L. contributed equally to this work. This work was supported by the National Research Foundation of Korea (NRF) grant funded by the Korea government (MSIT) (2018R1A4A1025986).

Conflict of Interest

The authors declare no conflict of interest.

Keywords

electronic skin, human–machine interfaces, robotics, tactile sensors, wearable electronics

Received: August 30, 2020
Revised: November 7, 2020
Published online:

[1] A. Chortos, J. Liu, Z. Bao, *Nat. Mater.* **2016**, *15*, 937.
[2] F. W. Clippinger, R. Avery, B. R. Titus, *Bull. Prosthet. Res.* **1974**, 247.
[3] X. Wang, L. Dong, H. Zhang, R. Yu, C. Pan, Z. L. Wang, *Adv. Sci.* **2015**, *2*, 1500169.
[4] D. J. Lipomi, M. Vosgueritchian, B. C. K. Tee, S. L. Hellstrom, J. A. Lee, C. H. Fox, Z. Bao, *Nat. Nanotechnol.* **2011**, *6*, 788.
[5] S. Kang, J. Lee, S. Lee, S. G. Kim, J. K. Kim, H. Algadi, S. Al-Sayari, D. E. Kim, D. E. Kim, T. Lee, *Adv. Electron. Mater.* **2016**, *2*, 1600356.
[6] Y. H. Jung, B. Park, J. U. Kim, T. Kim, *Adv. Mater.* **2019**, *31*, 1803637.
[7] M. Xie, K. Hisano, M. Zhu, T. Toyoshi, M. Pan, S. Okada, O. Tsutsumi, S. Kawamura, C. Bowen, *Adv. Mater. Technol.* **2019**, *4*, 1800626.
[8] S. Lim, D. Son, J. Kim, Y. B. Lee, J. K. Song, S. Choi, D. J. Lee, J. H. Kim, M. Lee, T. Hyeon, D. H. Kim, *Adv. Funct. Mater.* **2015**, *25*, 375.
[9] M. Zhu, Z. Sun, Z. Zhang, Q. Shi, T. He, H. Liu, T. Chen, C. Lee, *Sci. Adv.* **2020**, *6*, eaaz8693.
[10] T. Yang, D. Xie, Z. Li, H. Zhu, *Mater. Sci. Eng., R* **2017**, *115*, 1.
[11] J. Li, R. Bao, J. Tao, Y. Peng, C. Pan, *J. Mater. Chem. C* **2018**, *6*, 11878.
[12] C. Wang, L. Dong, D. Peng, C. Pan, *Adv. Intell. Syst.* **2019**, *1*, 1900090.
[13] J. C. Yang, J. Mun, S. Y. Kwon, S. Park, Z. Bao, S. Park, *Adv. Mater.* **2019**, *31*, 1904765.
[14] Y. Huang, X. Fan, S. C. Chen, N. Zhao, *Adv. Funct. Mater.* **2019**, *29*, 1808509.
[15] Y. Liu, R. Bao, J. Tao, J. Li, M. Dong, C. Pan, *Sci. Bull.* **2020**, *65*, 70.
[16] J. H. Lee, J. S. Heo, Y. J. Kim, J. Eom, H. J. Jung, J. W. Kim, I. Kim, H. H. Park, H. S. Mo, Y. H. Kim, S. K. Park, *Adv. Mater.* **2020**, *32*, 2000969.
[17] W. Zhong, C. Liu, Q. Liu, L. Piao, H. Jiang, W. Wang, K. Liu, M. Li, G. Sun, D. Wang, *ACS Appl. Mater. Interfaces* **2018**, *10*, 42706.
[18] S. Kim, M. Amjadi, T. I. Lee, Y. Jeong, D. Kwon, M. S. Kim, K. Kim, T. S. Kim, Y. S. Oh, I. Park, *ACS Appl. Mater. Interfaces* **2019**, *11*, 23639.
[19] B. Zhu, Z. Niu, H. Wang, W. R. Leow, H. Wang, Y. Li, L. Zheng, J. Wei, F. Huo, X. Chen, *Small* **2014**, *10*, 3625.
[20] M. Zhu, Y. Yue, Y. Cheng, Y. Zhang, J. Su, F. Long, X. Jiang, Y. Ma, Y. Gao, *Adv. Electron. Mater.* **2020**, *6*, 1901064.
[21] S. Pyo, J.-I. Lee, M.-O. Kim, T. Chung, Y. Oh, S.-C. Lim, J. Park, J. Kim, *J. Micromech. Microeng.* **2014**, *24*, 075012.
[22] S. Han, C. Liu, Z. Huang, J. Zheng, H. Xu, S. Chu, J. Wu, C. Liu, *Adv. Mater. Technol.* **2019**, *4*, 1800640.
[23] S. Pyo, J. Lee, W. Kim, E. Jo, J. Kim, *Adv. Funct. Mater.* **2019**, *29*, 1902484.
[24] H. Dai, E. T. Thostenson, *ACS Appl. Mater. Interfaces* **2019**, *11*, 48370.
[25] J. Choi, D. Kwon, K. Kim, J. Park, D. Del Orbe, J. Gu, J. Ahn, I. Cho, Y. Jeong, Y. Oh, I. Park, *ACS Appl. Mater. Interfaces* **2020**, *12*, 1698.
[26] B. W. An, S. Heo, S. Ji, F. Bien, J. U. Park, *Nat. Commun.* **2018**, *9*, 2458.
[27] J. Y. Yoo, M. H. Seo, J. S. Lee, K. W. Choi, M. S. Jo, J. B. Yoon, *Adv. Funct. Mater.* **2018**, *28*, 1804721.
[28] D. H. Ho, Q. Sun, S. Y. Kim, J. T. Han, D. H. Kim, J. H. Cho, *Adv. Mater.* **2016**, *28*, 2601.
[29] J. C. Yang, J. O. Kim, J. Oh, S. Y. Kwon, J. Y. Sim, D. W. Kim, H. B. Choi, S. Park, *ACS Appl. Mater. Interfaces* **2019**, *11*, 19472.
[30] W. Hu, X. Niu, R. Zhao, Q. Pei, *Appl. Phys. Lett.* **2013**, *102*, 083303.
[31] M. O. Kim, S. Pyo, Y. Oh, Y. Kang, K. H. Cho, J. Choi, J. Kim, *Smart Mater. Struct.* **2018**, *27*, 035001.
[32] T. Yang, H. Pan, G. Tian, B. Zhang, D. Xiong, Y. Gao, C. Yan, X. Chu, N. Chen, S. Zhong, L. Zhang, W. Deng, W. Yang, *Nano Energy* **2020**, *72*, 104706.
[33] M. Xie, Y. Zhang, M. J. Kraśny, C. Bowen, H. Khanbareh, N. Gathercole, *Energy Environ. Sci.* **2018**, *11*, 2919.
[34] F. R. Fan, Z. Q. Tian, Z. Lin Wang, *Nano Energy* **2012**, *1*, 328.
[35] J. Tao, R. Bao, X. Wang, Y. Peng, J. Li, S. Fu, C. Pan, Z. L. Wang, *Adv. Funct. Mater.* **2019**, *29*, 1806379.
[36] S. Park, H. Kim, M. Vosgueritchian, S. Cheon, H. Kim, J. H. Koo, T. R. Kim, S. Lee, G. Schwartz, H. Chang, Z. Bao, *Adv. Mater.* **2014**, *26*, 7324.
[37] K. Zhou, Y. Zhao, X. Sun, Z. Yuan, G. Zheng, K. Dai, L. Mi, C. Pan, C. Liu, C. Shen, *Nano Energy* **2020**, *70*, 104546.
[38] X. X. Zhu, X. S. Meng, S. Y. Kuang, X. Di Wang, C. F. Pan, G. Zhu, Z. L. Wang, *Nano Energy* **2017**, *41*, 387.
[39] X. Pu, M. Liu, X. Chen, J. Sun, C. Du, Y. Zhang, J. Zhai, W. Hu, Z. L. Wang, *Sci. Adv.* **2017**, *3*, e1700015.
[40] J. Huang, X. Yang, J. Yu, J. Han, C. Jia, M. Ding, J. Sun, X. Cao, Q. Sun, Z. L. Wang, *Nano Energy* **2020**, *69*, 104419.
[41] S. Pyo, M. O. Kim, D. S. Kwon, W. Kim, J. H. Yang, H. S. Cho, J. H. Lee, J. Kim, *Smart Mater. Struct.* **2020**, *29*, 055026.
[42] J. T. Kim, H. Choi, E. J. Shin, S. Park, I. G. Kim, *Sci. Rep.* **2018**, *8*, 16118.
[43] A. Alfadhel, M. A. Khan, S. Cardoso De Freitas, J. Kosel, *IEEE Sens. J.* **2016**, *16*, 8700.
[44] V. Amoli, J. S. Kim, S. Y. Kim, J. Koo, Y. S. Chung, H. Choi, D. H. Kim, *Adv. Funct. Mater.* **2020**, *30*, 1904532.
[45] E. S. Dellon, R. Mourey, A. L. Dellon, *Plast. Reconstr. Surg.* **1992**, *90*, 112.
[46] J. M. K. C. Craig James, *Somatosens. Mot. Res.* **1998**, *15*, 29.
[47] S. C. B. Mannsfeld, B. C. K. Tee, R. M. Stoltenberg, C. V. H. H. Chen, S. Barman, B. V. O. Muir, A. N. Sokolov, C. Reese, Z. Bao, *Nat. Mater.* **2010**, *9*, 859.
[48] G. Schwartz, B. C. K. Tee, J. Mei, A. L. Appleton, D. H. Kim, H. Wang, Z. Bao, *Nat. Commun.* **2013**, *4*, 1859.
[49] Z. Wang, S. Guo, H. Li, B. Wang, Y. Sun, Z. Xu, X. Chen, K. Wu, X. Zhang, F. Xing, L. Li, W. Hu, *Adv. Mater.* **2019**, *31*, 1805630.
[50] S. Jung, J. H. Kim, J. Kim, S. Choi, J. Lee, I. Park, T. Hyeon, D. H. Kim, *Adv. Mater.* **2014**, *26*, 4825.
[51] M. Ha, S. Lim, S. Cho, Y. Lee, S. Na, C. Baig, H. Ko, *ACS Nano* **2018**, *12*, 3964.
[52] Y. Luo, J. Shao, S. Chen, X. Chen, H. Tian, X. Li, L. Wang, D. Wang, B. Lu, *ACS Appl. Mater. Interfaces* **2019**, *11*, 17796.
[53] X. Chen, J. Shao, H. Tian, X. Li, C. Wang, Y. Luo, S. Li, *Adv. Mater. Technol.* **2020**, *5*, 2000046.
[54] B. Yin, X. Liu, H. Gao, T. Fu, J. Yao, *Nat. Commun.* **2018**, *9*, 5161.
[55] D. Kang, P. V. Pikhitsa, Y. W. Choi, C. Lee, S. S. Shin, L. Piao, B. Park, K. Y. Suh, T. Il Kim, M. Choi, *Nature* **2014**, *516*, 222.
[56] Y. W. Choi, D. Kang, P. V. Pikhitsa, T. Lee, S. M. Kim, G. Lee, D. Tahk, M. Choi, *Sci. Rep.* **2017**, *7*, 40116.
[57] S. H. Cho, S. W. Lee, S. Yu, H. Kim, S. Chang, D. Kang, I. Hwang, H. S. Kang, B. Jeong, E. H. Kim, S. M. Cho, K. L. Kim, H. Lee, W. Shim, C. Park, *ACS Appl. Mater. Interfaces* **2017**, *9*, 10128.
[58] Y. Lee, J. Park, S. Cho, Y. E. Shin, H. Lee, J. Kim, J. Myoung, S. Cho, S. Kang, C. Baig, H. Ko, *ACS Nano* **2018**, *12*, 4045.
[59] Y. Zang, F. Zhang, C. A. Di, D. Zhu, *Mater. Horiz.* **2015**, *2*, 140.
[60] L. Yang, Y. Liu, C. D. M. Filipe, D. Ljubic, Y. Luo, H. Zhu, J. Yan, S. Zhu, *ACS Appl. Mater. Interfaces* **2019**, *11*, 4318.

[61] G. Y. Bae, S. W. Pak, D. Kim, G. Lee, D. H. Kim, Y. Chung, K. Cho, *Adv. Mater.* **2016**, *28*, 5300.
[62] C. Jeong, J. S. Lee, B. Park, C. S. Hong, J. U. Kim, T. il Kim, *Adv. Mater.* **2019**, *31*, 1902689.
[63] Y. Pang, K. Zhang, Z. Yang, S. Jiang, Z. Ju, Y. Li, X. Wang, D. Wang, M. Jian, Y. Zhang, R. Liang, H. Tian, Y. Yang, T. L. Ren, *ACS Nano* **2018**, *12*, 2346.
[64] K. Wang, Z. Lou, L. Wang, L. Zhao, S. Zhao, D. Wang, W. Han, K. Jiang, G. Shen, *ACS Nano* **2019**, *13*, 9139.
[65] Y. Guo, M. Zhong, Z. Fang, P. Wan, G. Yu, *Nano Lett.* **2019**, *19*, 1143.
[66] W. Cheng, L. Yu, D. Kong, Z. Yu, H. Wang, Z. Ma, Y. Wang, J. Wang, L. Pan, Y. Shi, *IEEE Electron Device Lett.* **2018**, *39*, 1069.
[67] T. Li, L. Chen, X. Yang, X. Chen, Z. Zhang, T. Zhao, X. Li, J. Zhang, *J. Mater. Chem. C* **2019**, *7*, 1022.
[68] S. Chun, I. Y. Choi, W. Son, G. Y. Bae, E. J. Lee, H. Kwon, J. Jung, H. S. Kim, J. K. Kim, W. Park, *Adv. Funct. Mater.* **2018**, *28*, 6.
[69] S. G. Yoon, H. J. Koo, S. T. Chang, *ACS Appl. Mater. Interfaces* **2015**, *7*, 27562.
[70] J. Oh, J. O. Kim, Y. Kim, H. B. Choi, J. C. Yang, S. Lee, M. Pyatykh, J. Kim, J. Y. Sim, S. Park, *Small* **2019**, *15*, 1901744.
[71] L. Jin, A. Chortos, F. Lian, E. Pop, C. Linder, Z. Bao, W. Cai, *Proc. Natl. Acad. Sci. U. S. A.* **2018**, *115*, 1986.
[72] L. Ci, J. Suhr, V. Pushparaj, X. Zhang, P. M. Ajayan, *Nano Lett.* **2008**, *8*, 2762.
[73] K. Park, S. Kim, H. Lee, I. Park, J. Kim, *Sensors Actuators, A* **2019**, *295*, 541.
[74] M. Amjadi, Y. J. Yoon, I. Park, *Nanotechnology* **2015**, *26*, 375501.
[75] S. Sundaram, P. Kellnhofer, Y. Li, J. Y. Zhu, A. Torralba, W. Matusik, *Nature* **2019**, *569*, 698.
[76] J. J. Boland, *Nat. Mater.* **2010**, *9*, 790.
[77] C. Pan, L. Dong, G. Zhu, S. Niu, R. Yu, Q. Yang, Y. Liu, Z. L. Wang, *Nat. Photonics* **2013**, *7*, 752.
[78] S. Liu, L. Wang, X. Feng, Z. Wang, Q. Xu, S. Bai, Y. Qin, Z. L. Wang, *Adv. Mater.* **2017**, *29*, 1606346.
[79] S. Pyo, J. Choi, J. Kim, *Adv. Electron. Mater.* **2018**, *4*, 1700427.
[80] L. Nela, J. Tang, Q. Cao, G. Tulevski, S. J. Han, *Nano Lett.* **2018**, *18*, 2054.
[81] Y. J. Park, B. K. Sharma, S. M. Shinde, M. S. Kim, B. Jang, J. H. Kim, J. H. Ahn, *ACS Nano* **2019**, *13*, 3023.
[82] I. You, S. E. Choi, H. Hwang, S. W. Han, J. W. Kim, U. Jeong, *Adv. Funct. Mater.* **2018**, *28*, 1801858.
[83] C. Yeom, K. Chen, D. Kiriya, Z. Yu, G. Cho, A. Javey, *Adv. Mater.* **2015**, *27*, 1561.
[84] M. Park, M. S. Kim, Y. K. Park, J. H. Ahn, *Appl. Phys. Lett.* **2015**, *106*, 043502.
[85] S. Chen, M. Li, Y. Huang, H. Xu, G. Gu, X. Guo, *IEEE Trans. Electron Devices* **2020**, *67*, 2940.
[86] X. X. Zhu, Z. Bin Li, X. S. Li, L. Su, X. Y. Wei, S. Y. Kuang, B. W. Su, J. Yang, Z. L. Wang, G. Zhu, *Nano Energy* **2018**, *50*, 497.
[87] H. L. Wang, S. Y. Kuang, H. Y. Li, Z. L. Wang, G. Zhu, *Small* **2020**, *16*, 1906352.
[88] L. Viry, A. Levi, M. Totaro, A. Mondini, V. Mattoli, B. Mazzolai, L. Beccai, *Adv. Mater.* **2014**, *26*, 2659.
[89] Z. Yuan, G. Shen, C. Pan, Z. L. Wang, *Nano Energy* **2020**, *73*, 104764.
[90] J. I. Lee, S. Pyo, M. O. Kim, J. Kim, *Nanotechnology* **2018**, *29*, 055501.
[91] H. Chen, Z. Su, Y. Song, X. Cheng, X. Chen, B. Meng, Z. Song, D. Chen, H. Zhang, *Adv. Funct. Mater.* **2017**, *27*, 1604434.
[92] S. Peng, S. Wu, Y. Yu, B. Xia, N. H. Lovell, C. H. Wang, *ACS Appl. Mater. Interfaces* **2020**, *12*, 22179.
[93] J. Lee, H. Kwon, J. Seo, S. Shin, J. H. Koo, C. Pang, S. Son, J. H. Kim, Y. H. Jang, D. E. Kim, T. Lee, *Adv. Mater.* **2015**, *27*, 2433.
[94] Y. Joo, J. Yoon, J. Ha, T. Kim, S. Lee, B. Lee, C. Pang, Y. Hong, *Adv. Electron. Mater.* **2017**, *3*, 1600455.
[95] S. Lee, A. Reuveny, J. Reeder, S. Lee, H. Jin, Q. Liu, T. Yokota, T. Sekitani, T. Isoyama, Y. Abe, Z. Suo, T. Someya, *Nat. Nanotechnol.* **2016**, *11*, 472.
[96] J. Deng, W. Zhuang, L. Bao, X. Wu, J. Gao, B. Wang, X. Sun, H. Peng, *Carbon* **2019**, *149*, 63.
[97] D.-J. Won, D. Yoo, J. Kim, *ACS Appl. Electron. Mater.* **2020**, *2*, 846.
[98] Z. Wang, Y. Si, C. Zhao, D. Yu, W. Wang, G. Sun, *ACS Appl. Mater. Interfaces* **2019**, *11*, 27200.
[99] E. Davoodi, H. Montazerian, R. Haghniaz, A. Rashidi, S. Ahadian, A. Sheikhi, J. Chen, A. Khademhosseini, A. S. Milani, M. Hoorfar, E. Toyserkani, *ACS Nano* **2020**, *14*, 1520.
[100] J. Xiong, P. Cui, X. Chen, J. Wang, K. Parida, M.-F. Lin, P. S. Lee, *Nat. Commun.* **2018**, *9*, 4280.
[101] Y.-C. Lai, Y.-C. Hsiao, H.-M. Wu, Z. L. Wang, *Adv. Sci.* **2019**, *6*, 1801883.
[102] G. Y. Bae, J. T. Han, G. Lee, S. Lee, S. W. Kim, S. Park, J. Kwon, S. Jung, K. Cho, *Adv. Mater.* **2018**, *30*, 1803388.
[103] J. Park, M. Kim, Y. Lee, H. S. Lee, H. Ko, *Sci. Adv.* **2015**, *1*, e1500661.
[104] R. Y. Tay, H. Li, J. Lin, H. Wang, J. S. K. Lim, S. Chen, W. L. Leong, S. H. Tsang, E. H. T. Teo, *Adv. Funct. Mater.* **2020**, *30*, 1909604.
[105] C. Zhang, S. Liu, X. Huang, W. Guo, Y. Li, H. Wu, *Nano Energy* **2019**, *62*, 164.
[106] N. T. Tien, S. Jeon, D. Kim, T. Q. Trung, M. Jang, B. Hwang, K. Byun, J. Bae, E. Lee, J. B. Tok, *Adv. Mater.* **2014**, *26*, 796.
[107] S. Y. Kim, S. Park, H. W. Park, D. H. Park, Y. Jeong, D. H. Kim, *Adv. Mater.* **2015**, *27*, 4178.
[108] Z. Lei, P. Wu, *Nat. Commun.* **2018**, *9*, 1134.
[109] S. Choi, K. Yoon, S. Lee, H. J. Lee, J. Lee, D. W. Kim, M. S. Kim, T. Lee, C. Pang, *Adv. Funct. Mater.* **2019**, *29*, 1905808.
[110] T. Bu, T. Xiao, Z. Yang, G. Liu, X. Fu, J. Nie, T. Guo, Y. Pang, J. Zhao, F. Xi, C. Zhang, Z. L. Wang, *Adv. Mater.* **2018**, *30*, 1800066.
[111] T. Someya, Y. Kato, T. Sekitani, S. Iba, Y. Noguchi, Y. Murase, H. Kawaguchi, T. Sakurai, *Proc. Natl. Acad. Sci. U. S. A.* **2005**, *102*, 12321.
[112] Q. Hua, J. Sun, H. Liu, R. Bao, R. Yu, J. Zhai, C. Pan, Z. L. Wang, *Nat. Commun.* **2018**, *9*, 244.
[113] S. Zhao, R. Zhu, *Adv. Mater.* **2017**, *29*, 1606151.
[114] S. Gong, L. W. Yap, B. Zhu, Q. Zhai, Y. Liu, Q. Lyu, K. Wang, M. Yang, Y. Ling, D. T. H. Lai, F. Marzbanrad, W. Cheng, *Adv. Mater.* **2019**, *31*, 1903789.
[115] J. O. Kim, S. Y. Kwon, Y. Kim, H. B. Choi, J. C. Yang, J. Oh, H. S. Lee, J. Y. Sim, S. Ryu, S. Park, *ACS Appl. Mater. Interfaces* **2019**, *11*, 1503.
[116] M. Soni, R. Dahiya, *Philos. Trans. R. Soc., A* **2020**, *378*, 20190156.
[117] H. Yuan, T. Lei, Y. Qin, R. Yang, *Nano Energy* **2019**, *59*, 84.
[118] C. García Núñez, L. Manjakkal, R. Dahiya, *npj Flex. Electron.* **2019**, *3*, 1.
[119] Y. Zhou, J. He, H. Wang, K. Qi, N. Nan, X. You, W. Shao, L. Wang, B. Ding, S. Cui, *Sci. Rep.* **2017**, *7*, 12949.
[120] X. Chen, X. Li, J. Shao, N. An, H. Tian, C. Wang, T. Han, L. Wang, B. Lu, *Small* **2017**, *13*, 1604245.
[121] C. Yan, W. Deng, L. Jin, T. Yang, Z. Wang, X. Chu, H. Su, J. Chen, W. Yang, *ACS Appl. Mater. Interfaces* **2018**, *10*, 41070.
[122] M. O. Kim, S. Pyo, G. Song, W. Kim, Y. Oh, C. Park, C. Park, J. Kim, *Adv. Mater. Technol.* **2018**, *3*, 1800048.
[123] J. Qi, A. C. Wang, W. Yang, M. Zhang, C. Hou, Q. Zhang, Y. Li, H. Wang, *Nano Energy* **2020**, *67*, 104206.
[124] H. Zhang, H. Wang, J. Zhang, Z. Zhang, Y. Yu, J. Luo, S. Dong, *Sensors Actuators, A* **2020**, *302*, 111806.
[125] A. Nozariasbmarz, H. Collins, K. Dsouza, M. H. Polash, M. Hosseini, M. Hyland, J. Liu, A. Malhotra, F. M. Ortiz, F. Mohaddes, V. P. Ramesh, Y. Sargolzaeiaval, N. Snouwaert, M. C. Özturk, D. Vashaee, *Appl. Energy* **2020**, *258*, 114069.

[126] Z. L. Wang, G. Zhu, Y. Yang, S. Wang, C. Pan, *Mater. Today* **2012**, *15*, 532.
[127] C. Zheng, L. Xiang, W. Jin, H. Shen, W. Zhao, F. Zhang, C. an Di, D. Zhu, *Adv. Mater. Technol.* **2019**, *4*, 1900247.
[128] J. Oh, J. H. Kim, K. T. Park, K. Jo, J. C. Lee, H. Kim, J. G. Son, *Nanoscale* **2018**, *10*, 18370.
[129] J. Yuan, R. Zhu, *Appl. Energy* **2020**, *271*, 115250.
[130] H. Xue, Q. Yang, D. Wang, W. Luo, W. Wang, M. Lin, D. Liang, Q. Luo, *Nano Energy* **2017**, *38*, 147.
[131] Y. Yang, H. Zhang, G. Zhu, S. Lee, Z. H. Lin, Z. L. Wang, *ACS Nano* **2013**, *7*, 785.
[132] H. Guo, J. Wan, H. Wu, H. Wang, L. Miao, Y. Song, H. Chen, M. Han, H. Zhang, *ACS Appl. Mater. Interfaces* **2020**, *12*, 22357.
[133] X. Wang, W. Z. Song, M. H. You, J. Zhang, M. Yu, Z. Fan, S. Ramakrishna, Y. Z. Long, *ACS Nano* **2018**, *12*, 8588.
[134] Y. E. Shin, S. D. Sohn, H. Han, Y. Park, H. J. Shin, H. Ko, *Nano Energy* **2020**, *72*, 104671.
[135] K. Zhao, B. Ouyang, C. R. Bowen, Z. L. Wang, Y. Yang, *Nano Energy* **2020**, *71*, 104632.
[136] Z. Wu, Y. Wang, X. Liu, C. Lv, Y. Li, D. Wei, Z. Liu, *Adv. Mater.* **2019**, *31*, 1800716.
[137] X. Chen, N. S. Villa, Y. Zhuang, L. Chen, T. Wang, Z. Li, T. Kong, *Adv. Energy Mater.* **2020**, *10*, 1902769.
[138] D. Chen, K. Jiang, T. Huang, G. Shen, *Adv. Mater.* **2020**, *32*, 1901806.
[139] S. A. Hashemi, S. Ramakrishna, A. G. Aberle, *Energy Environ. Sci.* **2020**, *13*, 685.
[140] C. G. Núñez, W. T. Navaraj, E. O. Polat, R. Dahiya, *Adv. Funct. Mater.* **2017**, *27*, 1606287.
[141] C. I. Jang, K. S. Shin, M. J. Kim, K. S. Yun, K. H. Park, J. Y. Kang, S. H. Lee, *Appl. Phys. Lett.* **2016**, *108*, 103701.
[142] B. Nie, R. Huang, T. Yao, Y. Zhang, Y. Miao, C. Liu, J. Liu, X. Chen, *Adv. Funct. Mater.* **2019**, *29*, 1808786.
[143] G. H. Lee, J. K. Park, J. Byun, J. C. Yang, S. Y. Kwon, C. Kim, C. Jang, J. Y. Sim, J. G. Yook, S. Park, *Adv. Mater.* **2020**, *32*, 1906269.
[144] C. M. Boutry, L. Beker, Y. Kaizawa, C. Vassos, H. Tran, A. C. Hinckley, R. Pfattner, S. Niu, J. Li, J. Claverie, Z. Wang, J. Chang, P. M. Fox, Z. Bao, *Nat. Biomed. Eng.* **2019**, *3*, 47.
[145] L. Y. Chen, B. C. K. Tee, A. L. Chortos, G. Schwartz, V. Tse, D. J. Lipomi, H. S. P. Wong, M. V. McConnell, Z. Bao, *Nat. Commun.* **2014**, *5*, 5028.
[146] R. Nopper, R. Niekrawietz, L. Reindl, *IEEE Trans. Instrum. Meas.* **2010**, *59*, 2450.
[147] J. Zhu, J. J. Fox, N. Yi, H. Cheng, *ACS Appl. Mater. Interfaces* **2019**, *11*, 8867.
[148] H. Jeong, L. Wang, T. Ha, R. Mitbander, X. Yang, Z. Dai, S. Qiao, L. Shen, N. Sun, N. Lu, *Adv. Mater. Technol.* **2019**, *4*, 1900117.
[149] S. Han, J. Kim, S. M. Won, Y. Ma, D. Kang, Z. Xie, K. T. Lee, H. U. Chung, A. Banks, S. Min, S. Y. Heo, C. R. Davies, J. W. Lee, C. H. Lee, B. H. Kim, K. Li, Y. Zhou, C. Wei, X. Feng, Y. Huang, J. A. Rogers, *Sci. Transl. Med.* **2018**, *10*, eaan4950.
[150] H. U. Chung, B. H. Kim, J. Y. Lee, J. Lee, Z. Xie, E. M. Ibler, K. H. Lee, A. Banks, J. Y. Jeong, J. Kim, C. Ogle, D. Grande, Y. Yu, H. Jang, P. Assem, D. Ryu, J. W. Kwak, M. Namkoong, J. Bin Park, Y. Lee, D. H. Kim, A. Ryu, J. Jeong, K. You, B. Ji, Z. Liu, Q. Huo, X. Feng, Y. Deng, Y. Xu, K. I. Jang, J. Kim, Y. Zhang, R. Ghaffari, C. M. Rand, M. Schau, A. Hamvas, D. E. Weese-Mayer, Y. Huang, S. M. Lee, C. H. Lee, N. R. Shanbhag, A. S. Paller, S. Xu, J. A. Rogers, *Science* **2019**, *363*, eaau0780.
[151] Z. Xie, R. Avila, Y. Huang, J. A. Rogers, *Adv. Mater.* **2020**, *32*, 1902767.
[152] Y. R. Jeong, J. Kim, Z. Xie, Y. Xue, S. M. Won, G. Lee, S. W. Jin, S. Y. Hong, X. Feng, Y. Huang, J. A. Rogers, J. S. Ha, *NPG Asia Mater* **2017**, *9*, e443.
[153] I. Puchades, J. E. Rossi, C. D. Cress, E. Naglich, B. J. Landi, *ACS Appl. Mater. Interfaces* **2016**, *8*, 20986.
[154] F. Liu, Y. Chen, H. Song, F. Zhang, Z. Fan, Y. Liu, X. Feng, J. A. Rogers, Y. Huang, Y. Zhang, *Small* **2019**, *15*, 1804055.
[155] K. Meng, J. Chen, X. Li, Y. Wu, W. Fan, Z. Zhou, Q. He, X. Wang, X. Fan, Y. Zhang, J. Yang, Z. L. Wang, *Adv. Funct. Mater.* **2019**, *29*, 1806388.
[156] W. Zhong, Q. Liu, Y. Wu, Y. Wang, X. Qing, M. Li, K. Liu, W. Wang, D. Wang, *Nanoscale* **2016**, *8*, 12105.
[157] X. Tian, P. M. Lee, Y. J. Tan, T. L. Y. Wu, H. Yao, M. Zhang, Z. Li, K. A. Ng, B. C. K. Tee, J. S. Ho, *Nat. Electron.* **2019**, *2*, 243.
[158] S. Niu, N. Matsuhisa, L. Beker, J. Li, S. Wang, J. Wang, Y. Jiang, X. Yan, Y. Yun, W. Burnett, A. S. Y. Poon, J. B. H. Tok, X. Chen, Z. Bao, *Nat. Electron.* **2019**, *2*, 361.
[159] Q. Wu, Y. Qiao, R. Guo, S. Naveed, T. Hirtz, X. Li, Y. Fu, Y. Wei, G. Deng, Y. Yang, X. Wu, T. Ren, *ACS Nano* **2020**, *14*, 10104.
[160] W. Gao, S. Emaminejad, H. Y. Y. Nyein, S. Challa, K. Chen, A. Peck, H. M. Fahad, H. Ota, H. Shiraki, D. Kiriya, D. H. Lien, G. A. Brooks, R. W. Davis, A. Javey, *Nature* **2016**, *529*, 509.
[161] S. Emaminejad, W. Gao, E. Wu, Z. A. Davies, H. Y. Y. Nyein, S. Challa, S. P. Ryan, H. M. Fahad, K. Chen, Z. Shahpar, S. Talebi, C. Milla, A. Javey, R. W. Davis, *Proc. Natl. Acad. Sci. USA* **2017**, *114*, 4625.
[162] C. Bartolozzi, L. Natale, F. Nori, G. Metta, *Nat. Mater.* **2016**, *15*, 921.
[163] B. T. Nghiem, I. C. Sando, R. B. Gillespie, B. L. McLaughlin, G. J. Gerling, N. B. Langhals, M. G. Urbanchek, P. S. Cederna, *Plast. Reconstr. Surg.* **2015**, *135*, 1652.
[164] Y. C. Lai, J. Deng, R. Liu, Y. C. Hsiao, S. L. Zhang, W. Peng, H. M. Wu, X. Wang, Z. L. Wang, *Adv. Mater.* **2018**, *30*, 180114.
[165] C. M. Boutry, M. Negre, M. Jorda, O. Vardoulis, A. Chortos, O. Khatib, Z. Bao, *Sci. Robot.* **2018**, *3*, eaau6914.
[166] B. Oh, Y.-G. Park, H. Jung, S. Ji, W. H. Cheong, J. Cheon, W. Lee, J.-U. Park, *Soft Robot.* **2020**, *7*, 564.
[167] J. Ge, X. Wang, M. Drack, O. Volkov, M. Liang, G. S. Cañón Bermúdez, R. Illing, C. Wang, S. Zhou, J. Fassbender, M. Kaltenbrunner, D. Makarov, *Nat. Commun.* **2019**, *10*, 4405.
[168] Y. Li, Z. Cao, T. Li, F. Sun, Y. Bai, Q. Lu, S. Wang, X. Yang, M. Hao, N. Lan, *Research* **2020**, *2020*, 8910692.
[169] J. Kim, M. Lee, H. J. Shim, R. Ghaffari, H. R. Cho, D. Son, Y. H. Jung, M. Soh, C. Choi, S. Jung, K. Chu, D. Jeon, S. T. Lee, J. H. Kim, S. H. Choi, T. Hyeon, D. H. Kim, *Nat. Commun.* **2014**, *5*, 6747.
[170] P. Fattahi, G. Yang, G. Kim, M. R. Abidian, *Adv. Mater.* **2014**, *26*, 1846.
[171] B. C. K. Tee, A. Chortos, A. Berndt, A. K. Nguyen, A. Tom, A. McGuire, Z. C. Lin, K. Tien, W. G. Bae, H. Wang, P. Mei, H. H. Chou, B. Cui, K. Deisseroth, T. N. Ng, Z. Bao, *Science* **2015**, *350*, 313.
[172] C. Wan, G. Chen, Y. Fu, M. Wang, N. Matsuhisa, S. Pan, L. Pan, H. Yang, Q. Wan, L. Zhu, X. Chen, *Adv. Mater.* **2018**, *30*, 1801291.
[173] Y. Kim, A. Chortos, W. Xu, Y. Liu, J. Y. Oh, D. Son, J. Kang, A. M. Foudeh, C. Zhu, Y. Lee, S. Niu, J. Liu, R. Pfattner, Z. Bao, T. W. Lee, *Science* **2018**, *360*, 998.
[174] X. Zhang, Y. Zhuo, Q. Luo, Z. Wu, R. Midya, Z. Wang, W. Song, R. Wang, N. K. Upadhyay, Y. Fang, F. Kiani, M. Rao, Y. Yang, Q. Xia, Q. Liu, M. Liu, J. J. Yang, *Nat. Commun.* **2020**, *11*, 51.
[175] H. Tan, Q. Tao, I. Pande, S. Majumdar, F. Liu, Y. Zhou, P. O. Å. Persson, J. Rosen, S. van Dijken, *Nat. Commun.* **2020**, *11*, 1369.
[176] L. E. Osborn, A. Dragomir, J. L. Betthauser, C. L. Hunt, H. H. Nguyen, R. R. Kaliki, N. V. Thakor, *Sci. Robot.* **2018**, *3*, eaat3818.
[177] W. W. Lee, Y. J. Tan, H. Yao, S. Li, H. H. See, M. Hon, K. A. Ng, B. Xiong, J. S. Ho, B. C. K. Tee, *Sci. Robot.* **2019**, *4*, eaax2198.
[178] R. Ikeda, M. Cha, J. Ling, Z. Jia, D. Coyle, J. G. Gu, *Cell* **2014**, *157*, 664.

[179] R. Dahiya, N. Yogeswaran, F. Liu, L. Manjakkal, E. Burdet, V. Hayward, H. Jörntell, *Proc. IEEE* **2019**, *107*, 2016.
[180] S. Han, C. Liu, H. Xu, D. Yao, K. Yan, H. Zheng, H. J. Chen, X. Gui, S. Chu, C. Liu, *npj Flex. Electron.* **2018**, *2*, 16.
[181] X. Wang, Y. Zhang, X. Zhang, Z. Huo, X. Li, M. Que, Z. Peng, H. Wang, C. Pan, *Adv. Mater.* **2018**, *30*, 1706738.
[182] J. Byun, Y. Lee, J. Yoon, B. Lee, E. Oh, S. Chung, T. Lee, K. J. Cho, J. Kim, Y. Hong, *Sci. Robot.* **2018**, *3*, eaas9020.
[183] B. Dong, Y. Yang, Q. Shi, S. Xu, Z. Sun, S. Zhu, Z. Zhang, D.-L. Kwong, G. Zhou, K.-W. ANG, C. Lee, *ACS Nano* **2020**, *14*, 8915.
[184] X. Pu, H. Guo, J. Chen, X. Wang, Y. Xi, C. Hu, Z. L. Wang, *Sci. Adv.* **2017**, *3*, e1700694.
[185] X. Meng, Q. Cheng, X. Jiang, Z. Fang, X. Chen, S. Li, C. Li, C. Sun, W. Wang, Z. L. Wang, *Nano Energy* **2018**, *51*, 721.
[186] L. A. Jones, N. B. Sarter, *Human Factors* **2008**, *50*, 90.
[187] X. Yu, Z. Xie, Y. Yu, J. Lee, A. Vazquez-Guardado, H. Luan, J. Ruban, X. Ning, A. Akhtar, D. Li, B. Ji, Y. Liu, R. Sun, J. Cao, Q. Huo, Y. Zhong, C. M. Lee, S. Y. Kim, P. Gutruf, C. Zhang, Y. Xue, Q. Guo, A. Chempakasseril, P. Tian, W. Lu, J. Y. Jeong, Y. J. Yu, J. Cornman, C. S. Tan, B. H. Kim, K. H. Lee, X. Feng, Y. Huang, J. A. Rogers, *Nature* **2019**, *575*, 473.

Soonjae Pyo received the B.S. and Ph.D. degrees in mechanical engineering from Yonsei University, Seoul, South Korea, in 2009 and 2017, respectively. He is currently working as an assistant professor with the Department of Mechanical System Design Engineering, Seoul National University of Science and Technology. His research interests are modeling, design, and fabrication of nanomaterial-integrated micro/nanosystems.

Jaeyong Lee received the B.S. degree in mechanical engineering from Yonsei University, Seoul, South Korea, in 2017. He is currently an M.S. student in the Department of Mechanical Engineering at Yonsei University, South Korea, under the supervision of Prof. Jongbaeg Kim. His research interests are micro/nanoscience and human–machine interfaces.

Jongbaeg Kim received the B.S. degree in mechanical engineering from Yonsei University, Seoul, South Korea, in 1997, the M.S. degree in mechanical engineering from The University of Texas at Austin, Austin, TX, USA, in 1999, and the Ph.D. degree in mechanical engineering from the University of California at Berkeley, in 2004. From 2004 to 2005, he was with Dicon Fiberoptics, Inc., Richmond, CA, USA, where he designed and developed high-performance optical MEMS components for telecommunication applications. He joined Yonsei University, where he is currently a professor with the School of Mechanical Engineering. His research interests are modeling, design, fabrication of microsystems, and integrated nanostructures on MEMS.

